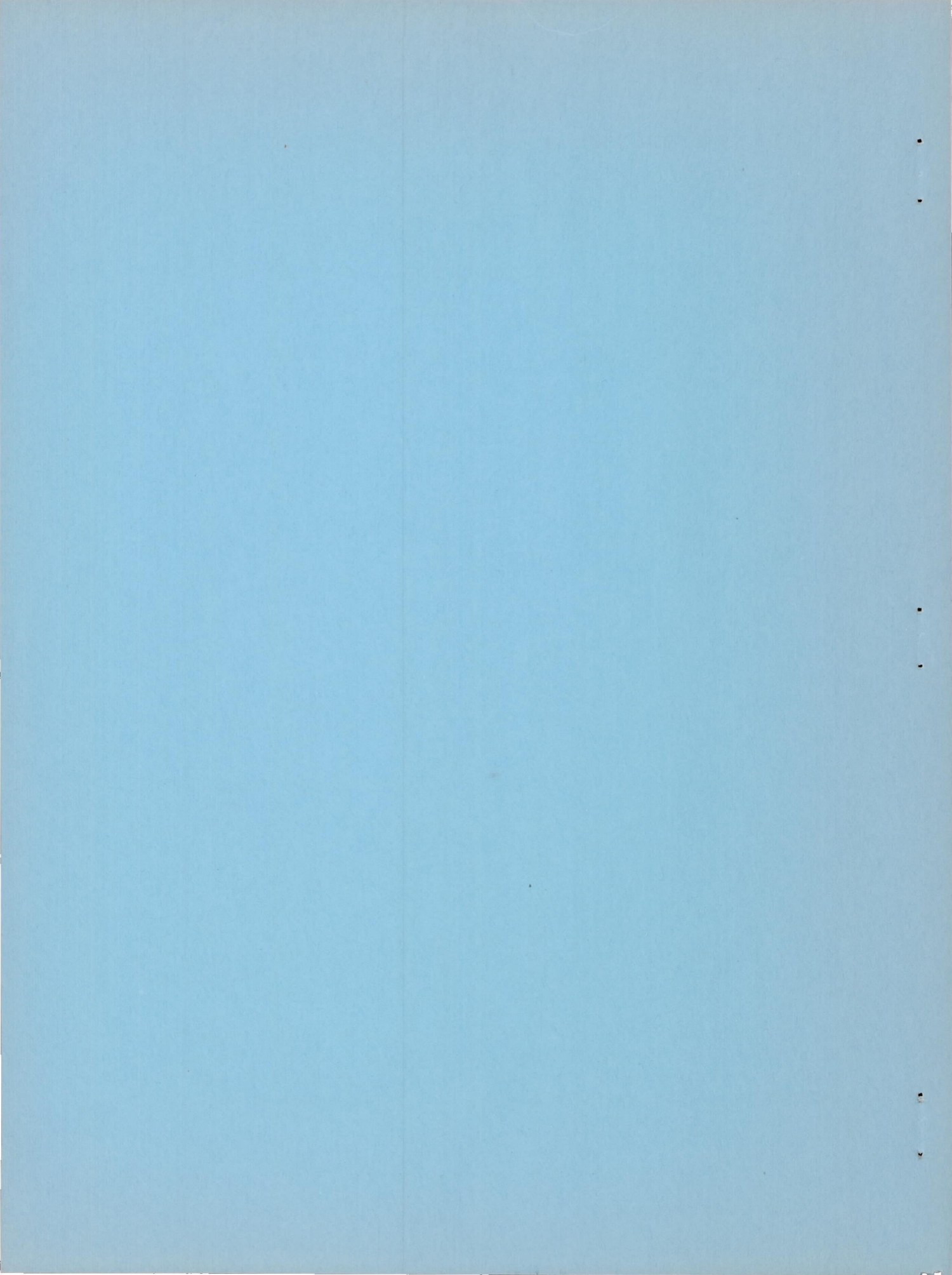RM A50K27b

NACA

RESEARCH MEMORANDUM

WIND-TUNNEL INVESTIGATION AT MACH NUMBERS FROM 0.50 TO 1.29

OF AN UNSWEPT, TAPERED WING OF ASPECT RATIO 2.67 WITH

LEADING- AND TRAILING-EDGE FLAPS - FLAPS

DEFLECTED IN COMBINATION

By Louis S. Stivers, Jr., and Alexander W. Malick

Ames Aeronautical Laboratory
Moffett Field, Calif.

NATIONAL ADVISORY COMMITTEE
FOR AERONAUTICS

WASHINGTON
February 26, 1951

NATIONAL ADVISORY COMMITTEE FOR AERONAUTICS

RESEARCH MEMORANDUM

WIND—TUNNEL INVESTIGATION AT MACH NUMBERS FROM 0.50 TO 1.29

OF AN UNSWEPT, TAPERED WING OF ASPECT RATIO 2.67 WITH

LEADING— AND TRAILING—EDGE FLAPS — FLAPS

DEFLECTED IN COMBINATION

By Louis S. Stivers, Jr., and Alexander W. Malick

SUMMARY

Aerodynamic characteristics of an unswept wing having an aspect
ratio of 2.67, a taper ratio of 0.5, and employing full—span,
25—percent—chord, plain, leading— and trailing—edge flaps have been
determined from wind—tunnel tests of a semispan model. Sections of the
wing were 8—percent chord thick from the 25— to the 75—percent—chord
points tapering to sharp leading and trailing edges. The data were
obtained for a range of angles of attack from —3° to 12° and for ranges
of leading—edge—flap deflection from —20° to 10° and of trailing—edge—
flap deflection from 0° to 60°. The Mach numbers ranged from about 0.50
to 0.95 and from 1.09 to 1.29 with corresponding Reynolds numbers vary-
ing from about 0.94×10^6 to 1.27×10^6.

The increments of lift coefficient produced by the combined deflec-
tions of the leading— and trailing—edge flaps were for the most part
approximately equal to the sum of the increments produced by the corre-
sponding deflections of each flap alone only at the supersonic Mach num-
bers and for the smaller flap deflections at a Mach number of 0.50.

Because of the large differences between the effects of Mach number
on the rates of change of hinge—moment coefficient with angle of attack
for the leading— and trailing—edge flaps, the degree of balance of the
control forces of one by those of the other, afforded by interlinking
the flaps, would vary over the ranges of test Mach number.

In contrast to the results of higher Reynolds number investigations
of similar low—aspect—ratio wings, the lift—drag ratios of the wing for
a given trailing—edge—flap deflection were not increased on the whole by
deflections of the leading—edge flap. The disagreement was believed to

have resulted from separation of the flow over the wing of the present
investigation due to the effects of the low test Reynolds numbers on the
particular wing section employed and of the relatively large flap–wing
gaps.

INTRODUCTION

Among the many problems associated with the application of low–
aspect–ratio unswept wings to aircraft designed for flight at supersonic
Mach numbers are those of increasing the lift coefficients of such wings
at moderate angles of attack and of providing sufficient control for
flight in the transonic Mach number range. As a solution to these prob-
lems for wings having sharp leading–edge airfoil sections, it has been
proposed to use both leading– and trailing–edge control surfaces. The
results of several investigations of low–aspect–ratio unswept wings hav-
ing various plan forms and section profiles, and employing leading– and
trailing–edge control surfaces in combination, have been reported in
references 1 to 4. With the aim of providing additional information
concerning the effectiveness and hinge–moment characteristics of such
control surfaces used in combination, an investigation has been made in
the Ames 1– by 3–1/2–foot high–speed wind tunnel of a semispan model of
a wing of aspect ratio 2.67 and taper ratio 0.5 equipped with full–span,
0.25 chord, plain, leading– and trailing–edge flaps. The aerodynamic
characteristics of the wing with the leading– and trailing–edge flaps
deflected separately have been reported in references 5 and 6, respec-
tively. It is the purpose of this report to present the aerodynamic
characteristics of the wing with the flaps deflected in combination for
Mach numbers from about 0.50 to 0.95 and from 1.09 to 1.29, with corre-
sponding Reynolds numbers varying from about 0.94×10^6 to 1.27×10^6.

NOTATION

c wing chord in streamwise direction

$\bar{c}$ mean aerodynamic chord of wing $\left(\dfrac{\int c^2 dy}{\int c \, dy} \right)$

C_D drag coefficient

C_{h_f} hinge–moment coefficient of trailing–edge flap, positive when
        moment tends to move trailing edge of flap downward
        $\left(\dfrac{\text{trailing–edge–flap hinge moment}}{2q \times \text{moment about hinge line of flap area behind hinge line}} \right)$

C_{h_n} hinge-moment coefficient of leading-edge flap, positive when
moment tends to move leading edge of flap upward

$$\left(\frac{\text{leading-edge-flap hinge moment}}{2q \times \text{moment about hinge line of flap area ahead of hinge line}} \right)$$

$\dfrac{dC_{h_f}}{d\alpha}$ rate of change of trailing-edge-flap hinge-moment coefficient
with angle of attack, per degree

$\dfrac{dC_{h_n}}{d\alpha}$ rate of change of leading-edge-flap hinge-moment coefficient
with angle of attack, per degree

C_L lift coefficient

C_m pitching-moment coefficient about lateral axis through quarter-
chord point of mean aerodynamic chord, with mean aerodynamic
chord as reference length

$\dfrac{L}{D}$ lift-drag ratio

q free-stream dynamic pressure

R Reynolds number based on mean aerodynamic chord

y spanwise distance measured from wing root-chord line

α wing angle of attack, degrees

α' wing geometric angle of attack, uncorrected for wind-tunnel jet-
boundary interference (at supersonic Mach numbers, equal to α),
degrees

δ_f trailing-edge-flap deflection, measured in plane normal to hinge
line, positive when trailing edge is below chord plane

δ_n leading-edge-flap deflection, measured in plane normal to hinge
line, positive when leading edge is above chord plane

DESCRIPTION OF APPARATUS

The investigation was conducted in the Ames 1- by 3-1/2-foot high-
speed wind tunnel, a single-return closed-throat tunnel vented to the
atmosphere in the settling chamber. To permit operation at both sub-
sonic and supersonic Mach numbers the tunnel was equipped with a
flexible-throat assembly which is illustrated in figure 1.

The semispan model used in the investigation was the same as that
employed in the investigations reported in references 5 and 6. The model
represented a complete wing with an aspect ratio of 2.67, a taper ratio
of 0.5, and an unswept 50-percent-chord line. The wing model was fitted
with full-span, 25-percent-chord, plain, leading- and trailing-edge
flaps, the hinge axes of which were coincident with the 25- and the
75-percent-chord lines of the wing. Sections of the wing in the stream-
wise direction were 8-percent chord thick from the 25- to the 75-percent-
chord points and tapered to sharp leading and trailing edges. The
leading- and trailing-edge angles thus formed were 18.2°. The gaps
between the flaps and the wing panel were approximately 1/32 inch. Plan
and section views of the wing model together with the principal dimen-
sions are shown in figure 2.

The model was mounted on an 18-inch-diameter balance plate in the
tunnel sidewall, as shown in the photograph of figure 3. Approximately
1/32-inch gaps were maintained between the roots of the undeflected
flaps and the balance plate. The face of the balance plate exposed to
the tunnel air stream was flush with the tunnel wall, and an approxi-
mately 1/16-inch annular gap existed between the periphery of the plate
and the tunnel wall. Flow through this gap from the outside atmosphere
was prevented by an external pressure-tight housing. The force reactions
on the wing and the hinge moments of the flaps were measured by electri-
cal resistance strain gages.

TESTS

Lift, drag, and pitching moments of the wing and hinge moments of
the leading- and trailing-edge flaps were determined as a function of
Mach number for constant geometric angles of attack from −3° to 12° and
for the following combinations of leading- and trailing-edge-flap deflec-
tions, with the flap-wing gaps unsealed:

δ_n, degrees	δ_f, degrees
5	10
10	20
−5	10
−10	20
−20	60

In addition, hinge moments of the undeflected leading-edge flap were
measured for trailing-edge-flap deflections of −10°, 10°, 20°, 40°, and
60°; hinge moments of the undeflected trailing-edge flap were measured
for leading-edge-flap deflections of 5°, 10°, −5°, −10°, and −20°.

The test Mach numbers ranged from about 0.50 to 0.95 and from 1.09 to 1.29 for the wing at the smaller angles of attack with the smaller flap deflections. No tests of the wing with flaps deflected could be made at Mach numbers between 0.95 and 1.09 because of choking conditions in the tunnel test section. The Reynolds numbers were based on the mean aerodynamic chord of the wing and varied from about 0.94×10^6 at a Mach number of 0.50 to a maximum of about 1.27×10^6 at a Mach number of 1.15, as shown in figure 4.

CORRECTIONS TO DATA

Wind—tunnel—wall interference corrections to the angles of attack and to the drag coefficients of the wing at subsonic Mach numbers were determined by the methods of reference 7. The following corrections, which are indicated in reference 8 to be independent of Mach number, were added:

$$\Delta \alpha \text{ (deg)} = 0.51 \ C_L$$

$$\Delta C_D = 0.0089 \ C_L^2$$

All the subsonic Mach number data have been corrected for model and wake blockage by the methods of reference 9. These blockage corrections vary with the measured drag coefficient but were generally small, never exceeding a value of 3 percent even for the highest drag coefficients.

Tare corrections determined with the wing held independently of the balance plate have been subtracted from the data at all Mach numbers. These corrections were found to be practically independent of angle of attack or flap deflection and are given in coefficient form as follows:

M	Lift	Drag	Pitching moment
0.50	0.018	0.031	0.006
.70	.015	.031	.004
.80	.014	.031	.003
.90	.013	.031	.001
.95	.017	.033	−.003
1.09	.001	.020	0
1.20	.005	.025	−.002
1.29	.003	.021	−.001

The pitching—moment data were obtained from the lift and drag reactions and are subject to the combined errors of the lift and drag measurements. Consequently, in the present report, the pitching—moment coefficients are regarded as being of qualitative rather than quantitative value.

The stream inclination at the model position was found to be suffi-
ciently small at all the test Mach numbers that no stream-angle correc-
tions to the angles of attack were necessary. Tunnel-wall boundary-
layer measurements made at Mach numbers from 0.50 to 1.20 with the tun-
nel empty have indicated the existence of a turbulent boundary layer with
a displacement thickness of about 0.12 inch at each Mach number. The
velocity in the boundary layer at each Mach number varied approximately
as the 1/10 power of the distance from the wall. The effect of possible
drainage of low-energy air from the tunnel-wall boundary layer by the
low induced pressures on the wing is unknown. It is felt that the pos-
sible flow of air around the gaps at the roots of the flaps and through
the gap between the balance plate and the tunnel wall would have had a
negligible effect on the measured data.

RESULTS AND DISCUSSION

The basic force and moment data for the wing with undeflected flaps,
gaps unsealed and sealed, are reproduced in graphical form from refer-
ences 5 and 6. The corresponding data for the wing with the leading-
and trailing-edge flaps deflected in combination are presented in
tables I to VII.

Lift Characteristics

The effects of Mach number on the lift coefficient of the wing with
flaps undeflected for various geometric angles of attack are shown in
figure 5, which has been reproduced from reference 6. Lift coefficient
as a function of angle of attack for the various combinations of flap
deflections is presented in figure 6. Corresponding lift-coefficient
data from references 5 and 6 for separate deflections of the leading-
and trailing-edge flaps (gaps unsealed) are reproduced in figure 7. From
a comparison of figures 6 and 7 it is observed that at the supersonic
Mach numbers the increments of lift coefficient produced by the combined
deflections of the flaps are for the most part approximately equal to
the sum of the increments which resulted from the separate deflections.
This result is also evident at a Mach number of 0.50 for the smaller flap
deflections, but not at the higher subsonic Mach numbers, where, for the
wing of the present investigation, the effects of boundary-layer separa-
tion would be expected to be severe.

It is noted further from a comparison of figures 6 and 7 that,
except for angles of attack greater than about 6° at the subsonic Mach
numbers, the lift coefficient of the wing for a given trailing-edge-flap

deflection is increased by a positive deflection (upward) of the leading-edge flap. A negative deflection of the leading-edge flap for a given trailing-edge-flap deflection reduced the lift coefficient of the wing at each angle of attack. This latter result is also apparent in the higher Reynolds number data (at low subsonic Mach numbers) of references 1 and 2 for comparable wings at angles of attack up to about 10°.

Increments of lift coefficient due to separate deflections of the leading- and trailing-edge flaps have been calculated for a Mach number of 0.50 using thin airfoil theory modified for the effects of aspect ratio and compressibility (see references 10 and 11), and also for a Mach number of 1.29 using linear theory. The increments for 10° deflections of the flaps are compared with the corresponding experimental values (gaps unsealed) in the following table:

| Mach number | Increments of lift coefficient | | | |
| | Leading-edge flap | | Trailing-edge flap | |
	Calculated	Experimental	Calculated	Experimental
0.50	0.03	0.06	0.33	0.11
1.29	.13	.11	.21	.09

Considerable disagreement is observed between the calculated and experimental lift-coefficient increments for the trailing-edge flap. It is believed that the differences were caused by separation of the flow over the flap and that this separation resulted from the effects of the unsealed gaps and of the low test Reynolds numbers on the particular wing section employed.

Hinge-Moment Characteristics

The effects of Mach number on the hinge-moment coefficients of the undeflected leading- and trailing-edge flaps with geometric angle of attack as a parameter are shown in figures 8 and 9. These figures have been reproduced from references 5 and 6.

Hinge-moment coefficients of the leading- and trailing-edge flaps as a function of angle of attack are presented in figure 10 for the various combinations of flap deflections. It may be seen in this figure that the variations with angle of attack of the leading-edge-flap hinge-moment coefficient are very marked at each Mach number and are much greater than those for the trailing-edge flap.

The variations of hinge-moment coefficient with angle of attack for separate deflections of the leading- and trailing-edge flaps are reproduced in figure 11 from references 5 and 6. A comparison of figures 10 and 11 reveals that at both subsonic and supersonic Mach numbers the hinge-moment coefficients of the leading-edge flap are not greatly affected by a deflection of the trailing-edge flap. Except for the 60° deflection, the hinge-moment coefficients of the trailing-edge flap are markedly decreased when the flap is deflected in combination with the leading-edge flap.

The effects of trailing-edge-flap deflection on the hinge-moment coefficients of the undeflected leading-edge flap, and the effects of leading-edge-flap deflection on the hinge-moment coefficients of the undeflected trailing-edge flap are presented in figures 12 and 13, respectively, for various geometric angles of attack.

The effects of Mach number on the rates of change of hinge-moment coefficient with angle of attack for the leading- and trailing-edge flaps are shown in figure 14 for an angle of attack of 0°. It may be seen in this figure that the effects of Mach number on $dC_{h_n}/d\alpha$ and $dC_{h_f}/d\alpha$ are markedly different. As a consequence, the degree of balance of the hinge moments of one flap by those of the other, accomplished by means of a linkage between the flaps, would vary over the ranges of test Mach number. In the investigation reported in reference 3 for a Mach number of 1.9 it was also found that such a procedure for effectively reducing the hinge moments would be limited. For purposes of comparison, the effects of Mach number on the rates of change of hinge-moment coefficient with angle of attack for separate deflections of the leading- and trailing-edge flaps have been reproduced in figure 15 from references 5 and 6.

Drag Characteristics

The effect of Mach number on the drag coefficients of the wing with undeflected flaps for various geometric angles of attack is shown in figure 16, which has been reproduced from reference 6. The variation of drag coefficient with lift coefficient for the various combinations of leading- and trailing-edge-flap deflections are presented in figure 17. Lift-drag ratio as a function of lift coefficient is shown in figure 18 for the various combinations of flap deflections (gaps unsealed). It is evident in this figure that the combined deflections of the flaps are effective in improving the lift-drag ratios of the wing only for the higher lift coefficients. A comparison of these lift-drag ratios with those provided by deflections of the trailing-edge flap alone (reference 6) indicates that the lift-drag ratio of the wing for a given trailing-edge-flap deflection is generally not increased by deflections of the leading-edge flap. (See also reference 5). This result, however,

is at variance with the results of investigations which were made at low subsonic Mach numbers and at Reynolds numbers from about 3×10^6 to 8×10^6, and reported in references 1 and 2. The disagreement is due principally to the relatively large drag-coefficient increments of the present investigation which resulted from deflections of the leading-edge flap. The large increments are believed to have resulted from separation of the flow due to the low Reynolds numbers and the particular wing section employed, as well as the relatively large flap-wing gaps.

Pitching-Moment Characteristics

The effect of Mach number on the pitching-moment coefficients of the wing with undeflected flaps for various geometric angles of attack is exhibited in figure 19, which has been reproduced from reference 6.

Pitching-moment coefficient as a function of lift coefficient is presented in figure 20 for the various combinations of flap deflections. Large variations in the location of the center of pressure for each combination of flap deflections are indicated in this figure.

CONCLUSIONS

An investigation of a semispan model of an unswept, tapered wing of aspect ratio 2.67 employing both leading- and trailing-edge flaps and having sharp leading-edge airfoil sections with a 0.08 thickness-chord ratio has been made at Mach numbers from about 0.50 to 0.95 and from 1.09 to 1.29 with corresponding Reynolds numbers varying from about 0.94×10^6 to 1.27×10^6. From the results of this investigation the following have been concluded:

1. At the supersonic Mach numbers the increments of lift coefficient provided by the various combinations of leading- and trailing-edge-flap deflections were, in general, approximately equal to the sum of the increments produced by the corresponding deflections of each flap alone. At the subsonic Mach numbers this result was apparent only for the smaller flap deflections at a Mach number of 0.50.

2. Because of the large differences between the effects of Mach number on the rates of change of hinge-moment coefficient with angle of attack for the leading- and trailing-edge flaps, the degree of balance of the control forces of one by those of the other, effected by inter-linking the flaps, would vary over the ranges of test Mach number.

3. In contrast to the results of higher Reynolds number investigations of similar low-aspect-ratio wings, the lift-drag ratios of the wing for a given trailing-edge-flap deflection were not increased for the most part by deflections of the leading-edge flap. The disagreement was believed to have resulted from separation of the flow over the wing of the present investigation due to the effects of the low test Reynolds numbers on the particular wing section employed and of the relatively large flap-wing gaps.

Ames Aeronautical Laboratory,
    National Advisory Committee for Aeronautics,
        Moffett Field, Calif.

REFERENCES

1. Lange, Roy H. and May, Ralph W., Jr.: Effect of Leading-Edge High-Lift Devices and Split Flaps on the Maximum-Lift and Lateral Characteristics of a Rectangular Wing of Aspect Ratio 3.4 With Circular-Arc Airfoil Sections at Reynolds Numbers from 2.9×10^6 to 8.4×10^6. NACA RM L8D30, 1948.

2. Johnson, Ben H., Jr., and Bandettini, Angelo: Investigation of a Thin Wing of Aspect Ratio 4 in the Ames 12-Foot Pressure Wind Tunnel. II - The Effect of Constant-Chord Leading- and Trailing-Edge Flaps on the Low-Speed Characteristics of the Wing. NACA RM A8F15, 1948.

3. Conner, D. William, and Mitchell, Meade H., Jr.: Control Effectiveness and Hinge-Moment Measurements at a Mach Number of 1.9 of a Nose Flap and Trailing-Edge Flap on a Highly Tapered Low-Aspect-Ratio Wing. NACA RM L8K17a, 1949.

4. Strass, H. Kurt: Free-Flight Investigation of the Rolling Effectiveness at High Subsonic, Transonic, and Supersonic Speeds of Leading-Edge and Trailing-Edge Ailerons in Conjunction with Tapered and Untapered Plan Forms. NACA RM L8E10, 1948.

5. Stivers, Louis S., Jr., and Malick, Alexander W.: Wind-Tunnel Investigation at Mach Numbers from 0.50 to 1.29 of an Unswept, Tapered Wing of Aspect Ratio 2.67 With Leading- and Trailing-Edge Flaps - Leading-Edge Flaps Deflected. NACA RM A50K10, 1950.

6. Stivers, Louis S., Jr., and Malick, Alexander W.: Wind-Tunnel Investigation at Mach Numbers from 0.50 to 1.29 of an Unswept Tapered Wing of Aspect Ratio 2.67 With Leading- and Trailing-Edge Flaps - Trailing-Edge Flaps Deflected. NACA RM A50J09b, 1950.

7. Glauert, H.: Wind—Tunnel Interference on Wings, Bodies, and Air—
    screws. R.& M. No. 1566, British, A.R.C., 1933.

8. Goldstein, S., and Young, A. D.: The Linear Perturbation Theory of
    Compressible Flow With Applications to Wind—Tunnel Interference.
    R.& M. No. 1909, British, A.R.C., July 6, 1943.

9. Herriot, John G.: Blockage Corrections for Three—Dimensional—Flow
    Closed—Throat Wind Tunnels, With Consideration of the Effects of
    Compressibility. NACA RM A7B28, 1947.

10. Perring, W. G. A.: The Theoretical Relationships for an Aerofoil
    With a Multiply Hinged Flap System. British R.& M. No. 1171,
    A.R.C., April, 1928.

11. DeYoung, John, and Harper, Charles W.: Theoretical Symmetric Span
    Loading at Subsonic Speeds for Wings Having Arbitrary Plan Form.
    NACA Rep. 921, 1949.

TABLE I.— BASIC AERODYNAMIC DATA; δ_n, 5° AND δ_f, 10°

M	α	C_L	C_D	C_m	C_{h_n}	C_{h_f}
0.51	-3.0	0.008	0.029	-0.025	0.075	-0.072
.72	-3.0	-.038	.041	-.005	.075	-.064
.82	-3.0	-.080	.046	.006	.076	-.049
.88	-3.1	-.118	.053	.015	.087	-.040
.91	-3.1	-.166	.059	.038	.090	-.023
.95	-3.1	-.127	- - -	.031	.087	-.020
1.09	-3.0	-.069	.087	.003	.097	-.080
1.20	-3.0	-.033	.093	.015	.163	-.096
1.29	-3.0	-.004	.080	.002	.051	-.095
.51	.1	.126	.038	-.030	.277	-.059
.72	.1	.118	.047	-.009	.323	-.063
.82	.1	.091	.045	-.005	.315	-.058
.91	0	.057	.050	.020	.340	-.052
.95	0	.052	.068	.014	.343	-.039
1.09	0	.100	.087	-.015	.306	-.088
1.20	0	.130	.090	-.011	.314	-.138
1.29	0	.143	.079	-.023	.192	-.163
.51	3.1	.281	.049	-.032	.541	-.073
.72	3.2	.300	.048	-.010	.549	-.076
.82	3.1	.283	.051	-.006	.602	-.072
.88	3.2	.296	.053	-.004	.574	-.071
1.09	3.0	.300	.088	-.028	.440	-.127
1.20	3.0	.302	.100	-.021	.402	-.163
1.29	3.0	.304	.096	-.036	.269	-.206
.51	6.2	.439	.091	-.082	.381	-.078
.72	6.3	.490	.088	-.067	.575	-.080
.82	6.3	.509	.095	-.027	.668	-.081
.88	6.3	.540	.093	-.024	.746	-.082
1.09	6.0	.514	.145	-.059	.572	-.191
1.20	6.0	.449	.132	-.047	.482	-.192
1.29	6.0	.438	.128	-.063	.333	-.234
.51	9.3	.479	.152	-.070	.530	-.094
.72	9.3	.520	.145	-.055	.548	-.101
.82	9.3	.561	.151	-.046	.577	-.115
.88	9.3	.572	.158	-.058	.589	-.134
.92	9.3	.659	.181	-.062	.807	-.153
1.20	9.0	.607	.179	-.077	.553	-.273
1.29	9.0	.576	.176	-.084	.400	-.280
.51	12.3	.530	.211	-.074	.530	-.106
.72	12.3	.520	.203	-.055	.506	-.117
.82	12.3	.585	.215	-.066	.543	-.145
.88	12.3	.634	.230	-.067	.559	-.181
.92	12.4	.756	.287	-.121	.646	-.258
1.20	12.0	.754	.247	-.118	.570	-.289

TABLE II.— BASIC AERODYNAMIC DATA; δ_n, 10° AND δ_f, 20°

M	α	C_L	C_D	C_m	c_{h_n}	c_{h_f}
0.51	−3.0	0.044	0.051	0.027	0.335	−0.099
.72	−3.0	.031	.053	.052	.395	−.085
.82	−3.0	.015	.053	.066	.422	−.074
.88	−3.0	−.008	.056	.083	.457	−.057
.91	−3.0	−.024	.064	.083	.478	−.068
.95	−3.0	−.010	.078	.088	.468	−.120
1.09	−3.0	.060	.110	.003	− − −	− − −
1.20	−3.0	.080	− − −	.001	.322	−.209
1.29	−3.0	.138	.115	−.017	.308	−.259
.51	.1	.245	.064	−.030	.267	−.131
.72	.1	.261	.073	−.021	.472	−.135
.82	.1	.248	.075	−.010	.570	−.137
.88	.1	.235	.080	.015	.683	−.126
.92	.1	.241	.089	.027	.674	−.140
1.09	0	.291	.132	−.032	.546	−.240
1.20	0	.268	.153	−.006	.406	−.272
1.29	0	.296	.127	−.042	.418	−.322
.51	3.2	.487	.096	−.098	.429	−.116
.72	3.3	.516	.115	−.084	.593	−.158
.83	3.3	.527	.122	−.062	.653	−.171
.88	3.3	.513	.128	−.055	.794	−.181
1.09	3.0	.534	.181	−.084	.667	−.321
1.20	3.0	.436	.190	−.038	.485	−.355
1.29	3.0	.440	.153	−.085	.442	−.407
.52	6.3	.590	.167	−.131	.592	−.166
.71	6.3	.653	.176	−.112	.659	−.187
.83	6.3	.655	.187	−.107	.662	−.209
1.20	6.0	.613	.241	−.075	.653	−.420
1.29	6.0	.585	.217	−.111	.510	−.469
.51	9.3	.595	.229	−.124	.653	−.189
.72	9.4	.680	.236	−.115	.621	−.210
.82	9.4	.690	.251	−.121	.633	−.241
.90	9.4	.745	.308	−.135	.994	−.305
.93	9.5	.890	.375	−.161	.886	−.239
1.20	9.0	.790	.263	−.149	.630	−.436
1.29	9.0	.704	.278	−.119	.560	−.496
.52	12.3	.608	.271	−.137	.462	−.221
.72	12.4	.719	.292	−.138	.614	−.226
.83	12.4	.803	.326	−.135	.625	−.311
.89	12.5	.887	.368	−.198	.680	−.389
1.20	12.0	.866	.332	−.192	.563	−.450

NACA

TABLE III.— BASIC AERODYNAMIC DATA; δ_n, $-5°$ AND δ_f, $10°$

M	α	C_L	C_D	C_m	c_{h_n}	c_{h_f}
0.51	−3.0	−0.035	0.043	−0.061	−0.468	−0.052
.71	−3.0	−.068	.043	−.060	−.531	−.057
.82	−3.0	−.086	.044	−.063	−.563	−.058
.87	−3.0	−.106	.044	−.063	−.575	−.057
.91	−3.1	−.112	.045	−.058	−.583	−.055
.94	−3.0	−.088	.048	−.132	−.563	−.056
1.09	−3.0	−.101	.078	−.072	−.468	−.127
1.20	−3.0	−.146	.088	−.063	−.474	−.113
1.29	−3.0	−.095	.081	−.070	−.375	−.104
.51	.1	.094	.041	−.069	−.199	−.158
.71	.1	.091	.041	−.074	−.248	−.062
.82	0	.085	.042	−.073	−.274	−.064
.87	0	.083	.043	−.070	−.303	−.060
.90	0	.086	.043	−.072	−.302	−.059
.93	0	.075	.046	.075	−.345	−.061
1.09	0	.087	.088	−.104	−.294	−.158
1.20	0	.046	.076	−.112	−.401	−.168
1.29	0	.058	.074	−.092	−.340	−.172
.51	3.1	.257	.053	−.076	.043	−.071
.71	3.1	.258	.054	−.077	.029	−.070
.82	3.1	.255	.054	−.070	.016	−.071
.88	3.1	.280	.057	−.075	−.005	−.070
91	3.1	.285	062	−.081	−.021	−.077
.94	3.1	.273	.067	−.087	−.031	−.091
1.09	3.0	.278	.075	−.127	−.098	−.183
1.20	3.0	.211	.088	−.115	−.220	−.201
1.29	3.0	.210	.088	−.107	−.226	−.220
.51	6.2	.385	.081	−.071	.245	−.077
.71	6.2	.388	.081	−.067	.220	−.081
.82	6.2	.385	.084	−.066	.183	−.084
.88	6.2	.420	.090	−.074	.151	−.088
.91	6.2	.440	.099	−.081	.144	−.104
.94	6.2	.450	.112	−.098	.123	−.139
1.09	6.0	.440	.138	−.133	.081	−.219
1.20	6.0	.369	.115	−.134	−.073	−.241
1.29	6.0	.351	.112	−.113	−.107	−.259
.51	9.2	.466	.116	−.072	.389	−.097
.72	9.2	.469	.118	−.061	.368	−.095
.82	9.3	.489	.121	−.060	.374	−.105
.88	9.3	.544	.122	−.062	.357	−.115
.92	9.3	.608	.155	−.090	.338	−.158
.95	9.3	.624	.187	−.137	.313	−.248
1.20	9.0	.507	.148	−.119	.078	−.265
1.29	9.0	.497	.147	−.126	.058	−.293
.51	12.3	.512	.171	−.075	.446	−.126
.72	12.3	.508	.174	−.069	.398	−.121
.82	12.3	.541	.180	−.068	.408	−.137
.88	12.3	.601	.191	−.072	.435	−.157
.92	12.4	.709	.212	−.108	.498	−.196
1.20	12.0	.670	.191	−.144	.214	−.289
1.29	12.0	.646	.199	−.139	.161	−.326

NACA

TABLE IV.— BASIC AERODYNAMIC DATA; δ_n, —10° AND δ_f, 20°

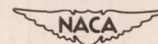| M	α	C_L	C_D	C_m	C_{h_n}	C_{h_f}
0.51	−3.0	0.004	0.030	−0.083	−0.658	−0.118
.72	−3.0	−.025	.047	−.073	−.645	−.118
.82	−3.0	−.052	.055	−.070	−.658	−.122
1.09	−3.0	−.016	.138	−.176	−.760	−.271
1.20	−3.0	−.065	− − −	−.146	−.648	−.273
1.29	−3.0	−.053	.134	−.160	−.549	−.286
.51	.1	−.175	.082	−.175	−.414	−.102
.72	.1	−.176	.087	−.176	−.436	−.179
.82	.1	−.182	.090	−.182	−.495	−.197
.88	.1	−.196	.105	−.196	−.611	−.223
1.09	0	.214	.124	−.206	−.666	−.301
1.20	0	.118	.131	−.193	−.677	−.367
1.29	0	.145	.129	−.167	−.540	−.375
.51	3.2	.331	.091	−.140	−.212	−.156
.72	3.2	.318	.097	−.135	−.304	−.166
.82	3.2	.329	.105	−.147	−.363	−.187
1.09	3.0	.407	.142	−.227	−.502	−.334
1.20	3.0	.316	.148	−.227	−.604	−.395
1.29	3.0	.277	.146	−.234	−.465	−.414
.51	6.2	.387	.132	−.143	−.031	−.181
.71	6.2	.410	.141	−.151	−.077	−.190
.82	6.2	.441	.149	−.169	−.108	−.210
1.20	6.0	.489	.174	−.195	−.385	−.407
1.29	6.0	.440	.179	−.247	−.311	−.425
.51	9.2	.444	.162	−.133	.138	−.183
.72	9.2	.467	.176	−.137	.082	−.196
.82	9.3	.502	.185	−.198	.052	−.224
1.20	9.0	.618	.218	−.197	−.196	−.431
1.29	9.0	.579	.222	−.225	−.119	−.447
.51	12.3	.492	.203	−.141	.285	−.190
.72	12.3	.521	.216	−.142	.229	−.203
.82	12.3	.579	.229	−.157	.203	−.238
1.20	12.0	.723	.280	−.209	−.017	−.452
1.29	12.0	.700	.277	−.209	.042	−.477

NACA

TABLE V.— BASIC AERODYNAMIC DATA; δ_n, -20° and δ_f, 60°

M	α	C_L	C_D	C_m	C_{h_n}	C_{h_f}
0.51	−2.9	0.212	0.204	−0.173	−0.597	−0.358
.72	−2.9	.190	.226	−.173	−.666	−.374
.82	−2.9	.153	.291	−.168	−.723	−.376
.89	−2.9	.138	.277	−.173	−.764	−.412
.93	−2.9	.138	.354	−.191	−.824	−.525
.51	.3	.479	.238	−.207	−.536	−.444
.72	.2	.428	.252	−.208	−.537	−.454
.83	.2	.393	.269	−.200	−.571	−.466
.89	.2	.375	.299	−.212	−.597	−.501
.91	.2	.377	.386	−.237	−.611	−.636
.51	3.4	.701	.287	−.256	−.540	−.503
.72	3.3	.662	.302	−.257	−.543	−.527
.83	3.3	.607	.315	−.251	−.545	−.534
.89	3.3	.626	.340	−.264	−.579	−.583
.92	3.3	.630	.441	−.288	−.597	−.715
.51	6.4	.713	.342	−.303	−.458	−.522
.72	6.4	.732	.362	−.315	−.459	−.555
.83	6.4	.742	.383	−.321	−.476	−.584
.89	6.4	.836	.455	−.361	−.524	−.692
.91	6.4	.890	.530	−.383	−.537	−.778
.52	9.4	.701	.376	−.243	−.322	−.534
.72	9.4	.752	.416	−.259	−.344	−.581
.83	9.4	.775	.436	−.279	−.382	−.615
.90	9.5	.973	.622	−.347	−.449	−.830
.51	12.4	.748	.416	−.222	−.201	−.545
.72	12.4	.791	.457	−.244	−.174	−.586
.83	12.4	.831	.498	−.268	−.216	−.634
.89	12.5	1.039	.682	−.374	−.287	−.816

NACA

TABLE VI.— BASIC HINGE—MOMENT COEFFICIENTS OF UNDEFLECTED LEADING—EDGE FLAP FOR VARIOUS DEFLECTIONS OF TRAILING—EDGE FLAP

| $\delta_f = -10°$			$\delta_f = 10°$			$\delta_f = 20°$		
M	α	c_{h_n}	M	α	c_{h_n}	M	α	c_{h_n}
0.51	-3.1	-0.141	0.51	-3.0	-0.094	0.51	-3.0	-0.063
.72	-3.1	-.156	.72	-3.0	-.118	.72	-3.0	-.086
.82	-3.1	-.158	.81	-3.0	-.144	.82	-3.0	-.120
.86	-3.2	-.140	.87	-3.1	-.140	.88	-3.0	-.149
.91	-3.2	-.135	.91	-3.1	-.131	.91	-3.0	-.165
.93	-3.1	-.123	.94	-3.1	-.117	.94	-3.0	-.173
.98	-3.2	-.114	1.09	-3.0	-.151	1.09	-3.0	-.154
1.09	-3.0	-.134	1.20	-3.0	-.214	1.20	-3.0	-.236
1.20	-3.0	-.164	1.29	-3.0	-.158	1.29	-3.0	-.230
1.29	-3.0	-.109						
.51	-.1	.025	.51	.1	.100	.51	.1	.098
.72	-.1	.024	.72	.1	.098	.72	.1	.107
.81	0	.029	.81	0	.092	.82	.1	.112
.86	0	.028	.88	0	.093	.88	.1	.101
.91	0	.034	.91	0	.092	.91	.1	.094
.94	0	.023	.94	0	.088	.94	.1	.087
.98	-.1	.036	1.09	0	.110	1.09	0	.043
1.09	0	.036	1.20	0	-.064	1.20	0	-.090
1.20	0	0	1.29	0	-.050	1.29	0	-.113
1.29	0	.026						
.51	3.0	.191	.51	3.1	.324	.51	3.2	.345
.72	3.0	.229	.72	3.1	.375	.72	3.2	.375
.81	3.0	.226	.81	3.1	.366	.82	3.2	.348
.86	3.1	.224	.88	3.2	.355	.88	3.2	.326
.91	3.1	.216	.90	3.2	.342	.91	3.2	.310
.96	3.1	.201	.94	3.1	.327	.95	3.3	.293
1.09	3.0	.216	1.09	3.0	.198	1.09	3.0	.213
1.20	3.0	.115	1.20	3.0	.074	1.20	3.0	.057
1.29	3.0	.139	1.29	3.0	.096	1.29	3.0	.029
.51	6.1	.326	.51	6.2	.278	.51	6.3	.387
.72	6.1	.344	.72	6.2	.350	.72	6.3	.423
.82	6.2	.361	.81	6.2	.369	.83	6.3	.520
.88	6.2	.361	.88	6.3	.357	.88	6.4	.486
.92	6.2	.339	.91	6.3	.348	.92	6.4	.450
.97	6.2	.318	.95	6.3	.306	.95	6.4	.428
1.09	6.0	.394	1.09	6.0	.380	1.20	6.0	.205
1.20	6.0	.263	1.20	6.0	.220	1.29	6.0	.168
1.29	6.0	.242	1.29	6.0	.241			
.51	9.1	.478	.52	9.3	.262	.51	9.3	.380
.72	9.2	.542	.72	9.3	.357	.73	9.3	.399
.82	9.2	.596	.82	9.3	.420	.81	9.4	.436
.88	9.3	.661	.88	9.3	.521	.88	9.4	.512
.91	9.3	.619	.91	9.3	.488	.93	9.5	.557
.95	9.3	.595	.94	9.4	.457	.94	9.5	.537
1.20	9.0	.342	.96	9.4	.444	1.20	9.0	.313
1.29	9.0	.318	1.20	9.0	.312	1.29	9.0	.246
			1.29	9.0	.313			
.51	12.1	.343	.51	12.3	.489	.53	12.3	.388
.72	12.2	.341	.72	12.3	.460	.72	12.4	.389
.82	12.2	.400	.82	12.3	.484	.82	12.4	.413
.89	12.2	.423	.89	12.3	.499	.88	12.4	.449
.92	12.2	.464	.92	12.4	.550	.92	12.5	.483
1.20	12.0	.413	1.20	12.0	.380	1.20	12.0	.372
1.29	12.0	.374	1.29	12.0	.361	1.29	12.0	.298

NACA
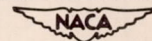
TABLE VI.— CONCLUDED

$\delta_f = 40°$			$\delta_f = 60°$		
M	α	c_{h_n}	M	α	c_{h_n}
0.51	−2.8	−0.070	0.51	−2.7	0
.72	−2.8	−.074	.72	−2.8	0
.82	−2.8	−.094	.82	−2.8	−.010
.88	−2.9	−.113	.89	−2.8	−.033
.51	.3	.126	.51	.3	.164
.72	.3	.112	.72	.3	.186
.82	.3	.099	.82	.3	.160
.88	.3	.083			
.92	.3	.062			
.51	3.3	.312	.51	3.4	.333
.72	3.3	.332	.72	3.4	.338
.83	3.4	.303	.82	3.4	.333
.89	3.4	.269	.88	3.4	.314
.93	3.4	.244			
.51	6.4	.395	.51	6.5	.471
.72	6.4	.393	.72	6.5	.448
.83	6.5	.426	.82	6.5	.425
.89	6.5	.475	.89	6.5	.407
.93	6.5	.447			
.51	9.5	.477	.51	9.5	.543
.72	9.5	.465	.72	9.5	.537
.82	9.5	.451	.83	9.5	.493
.89	9.5	.447	.90	9.6	.473
.51	12.5	.495	.51	12.5	.594
.72	12.5	.491	.72	12.5	.532
.83	12.5	.519	.83	12.5	.556
.90	12.6	.507			
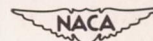
TABLE VII.— BASIC HINGE—MOMENT COEFFICIENTS OF UNDEFLECTED TRAILING—
EDGE FLAP FOR VARIOUS DEFLECTIONS OF LEADING—EDGE FLAP

$\delta_n = 5^\circ$			$\delta_n = 10^\circ$			$\delta_n = -5^\circ$		
M	α	c_{h_f}	M	α	c_{h_f}	M	α	c_{h_f}
0.51	−3.1	0.006	0.51	−3.0	−0.008	0.51	−3.1	−0.014
.72	−3.0	−.001	.72	−3.0	−.008	.72	−3.1	−.018
.82	−3.0	−.011	.82	−2.9	−.012	.82	−3.1	−.017
.88	−3.1	−.034	1.09	−3.0	−.047	.87	−3.1	−.035
.91	−3.0	−.076	1.20	−3.0	.019	.91	−3.1	−.039
.94	−3.0	−.085	1.29	−3.0	.043	.95	−3.1	−.071
1.09	−3.0	0				1.09	−3.0	−.021
1.20	−3.0	.016	.51	0	−.007	1.20	−3.0	.015
1.29	−3.0	.036	.72	0	−.011	1.29	−3.0	.025
			.82	.1	−.012			
.51	0	−.012	1.09	0	−.053	.51	0	.020
.72	0	−.004	1.20	0	−.006	.72	0	.031
.82	0	−.005	1.29	0	.007	.82	0	.044
.87	0	−.012				.88	0	.034
.91	0	−.035	.51	3.1	0	.91	0	.046
.95	0	−.068	.72	3.1	.001	.94	0	.086
1.09	0	−.005	.82	3.1	.002	1.09	0	.004
1.20	0	−.009	1.09	3.0	−.037	1.20	0	−.007
1.29	0	.005	1.20	3.0	−.014	1.29	0	−.001
			1.29	3.0	−.022			
.51	3.1	.003				.51	3.0	−.012
.72	3.1	.002	.51	6.2	.004	.72	3.0	−.008
.82	3.1	.002	.72	6.2	.005	.82	3.0	.007
.87	3.1	−.004	.82	6.2	.016	.88	3.1	−.003
.91	3.1	−.006	1.20	6.0	−.004	.91	3.1	.003
.95	3.1	−.015	1.29	6.0	−.081	.94	3.1	.017
1.09	3.0	−.004				1.09	3.0	.033
1.20	3.0	−.009	.51	9.2	−.009	1.20	3.0	−.022
1.29	3.0	−.023	.72	9.2	−.001	1.29	3.0	−.036
			.83	9.1	.049			
.51	6.2	.002	1.20	9.0	−.005	.51	6.1	−.018
.72	6.2	.005	1.29	9.0	−.125	.71	6.1	−.001
.83	6.2	.004				.81	6.1	.015
.89	6.2	.017	.51	12.2	−.020	.88	6.1	.082
.91	6.2	.022	.72	12.2	−.006	.90	6.1	.082
.95	6.2	.045	.82	12.2	.065	.95	6.1	.054
1.09	6.0	.030	1.29	12.0	−.177	.96	6.2	.013
1.20	6.0	−.013				1.09	6.0	.026
1.29	6.0	−.058				1.20	6.0	−.044
						1.29	6.0	−.074
.51	9.2	.002						
.72	9.2	.006				.51	9.2	0
.82	9.2	.042				.72	9.2	.006
.88	9.2	.075				.82	9.1	.044
.91	9.3	.074				.88	9.1	.105
.95	9.3	.033				.92	9.2	.090
1.20	9.0	−.020				.95	9.2	.021
1.29	9.0	−.089				1.20	9.0	−.045
						1.29	9.0	−.090
1.20	12.0	−.033				1.20	12.0	−.044
1.29	12.0	−.116				1.29	12.0	−.107

NACA
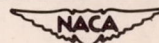
TABLE VII.— CONCLUDED.

$\delta_n = -10°$			$\delta_n = -20°$		
M	α	c_{h_f}	M	α	c_{h_f}
0.51	-3.1	0.005	0.51	-3.1	-0.025
.72	-3.1	.002	.72	-3.1	-.016
.82	-3.1	.002	.82	-3.1	-.013
1.09	-3.0	.021	.87	-3.1	-.013
1.20	-3.0	.010	.90	-3.1	-.016
1.29	-3.0	.011	.94	-3.2	-.084
.51	0	.006	.51	-.1	-.027
.72	0	.009	.71	-.1	-.016
.82	.1	.014	.82	-.1	-.013
1.09	0	.024	.87	-.1	-.016
1.20	0	.003	.91	-.1	-.006
1.29	0	.005	.94	-.1	.018
.51	3.0	.010	.51	3.0	.005
.72	3.0	.015	.72	3.0	.009
.82	3.0	.033	.82	2.9	.027
1.09	3.0	.024	.88	2.9	.040
1.20	3.0	-.018	.91	2.9	.066
1.29	3.0	-.036	.95	2.9	.073
.51	6.1	-.006	.51	6.1	-.025
.72	6.1	.001	.72	6.0	-.017
.82	6.0	.042	.82	6.0	-.013
1.09	6.0	.032	.88	6.0	.007
1.20	6.0	-.030	.91	6.0	.017
1.29	6.0	-.069	.95	6.1	-.008
.51	9.1	-.028	.51	9.1	-.047
.72	9.1	-.012	.71	9.1	-.025
.82	9.1	-.071	.82	9.0	.009
1.20	9.0	-.048	.87	9.0	.062
1.29	9.0	-.097	.91	9.0	.048
			.95	9.1	-.011
.51	12.1	-.043			
.72	12.1	-.023	.51	12.1	-.051
.82	12.1	-.016	.71	12.1	-.024
1.20	12.0	-.050	.82	12.1	.048
1.29	12.0	-.124	.88	12.1	.065
			.90	12.1	.044
			.94	12.2	-.029

NACA

Plate adjustment
mechanism

Airflow

Model
location

Flexible plate
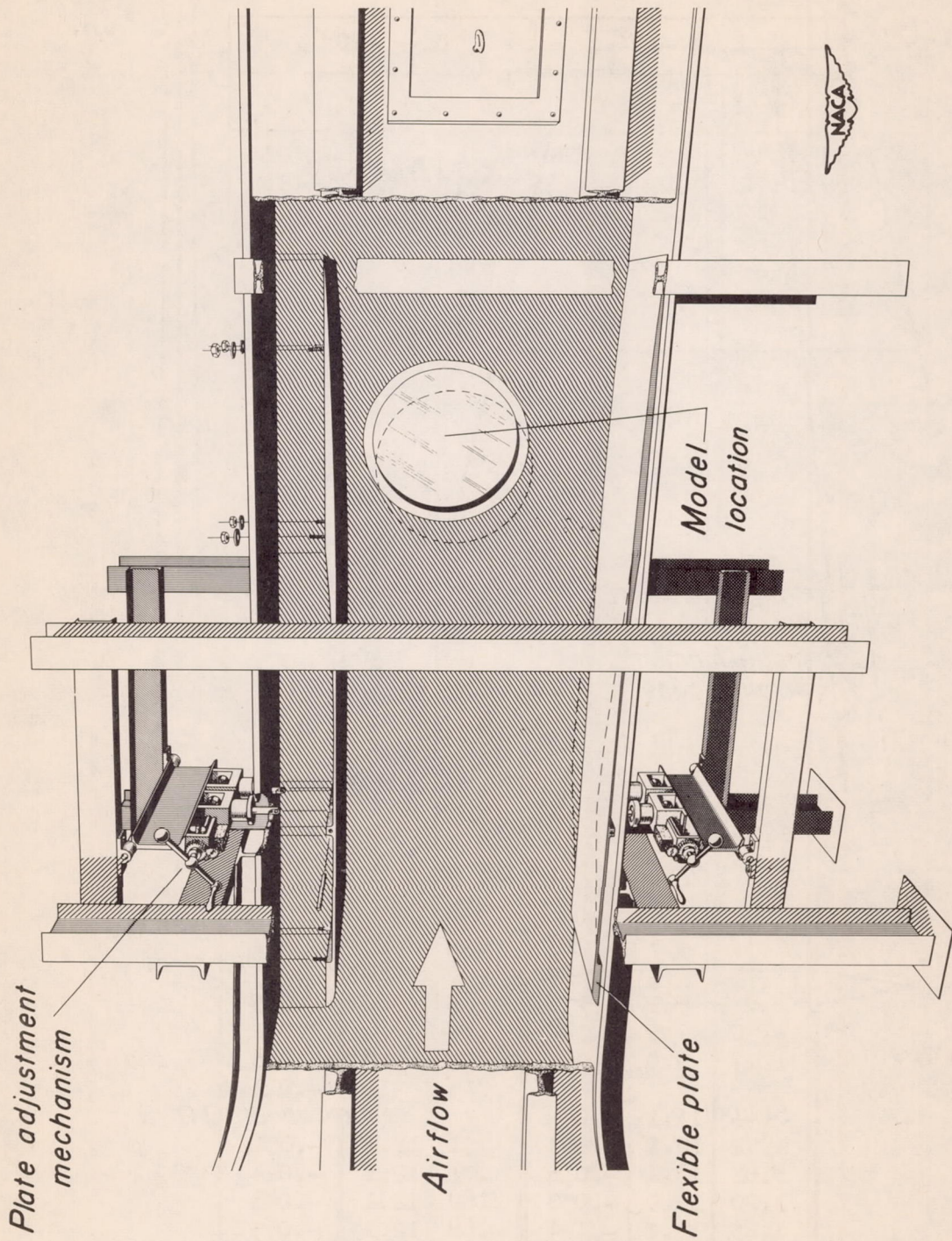
Figure I.— Illustration of the flexible—throat mechanism in the Ames I—by $3\frac{1}{2}$—foot
high-speed wind tunnel.
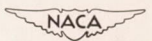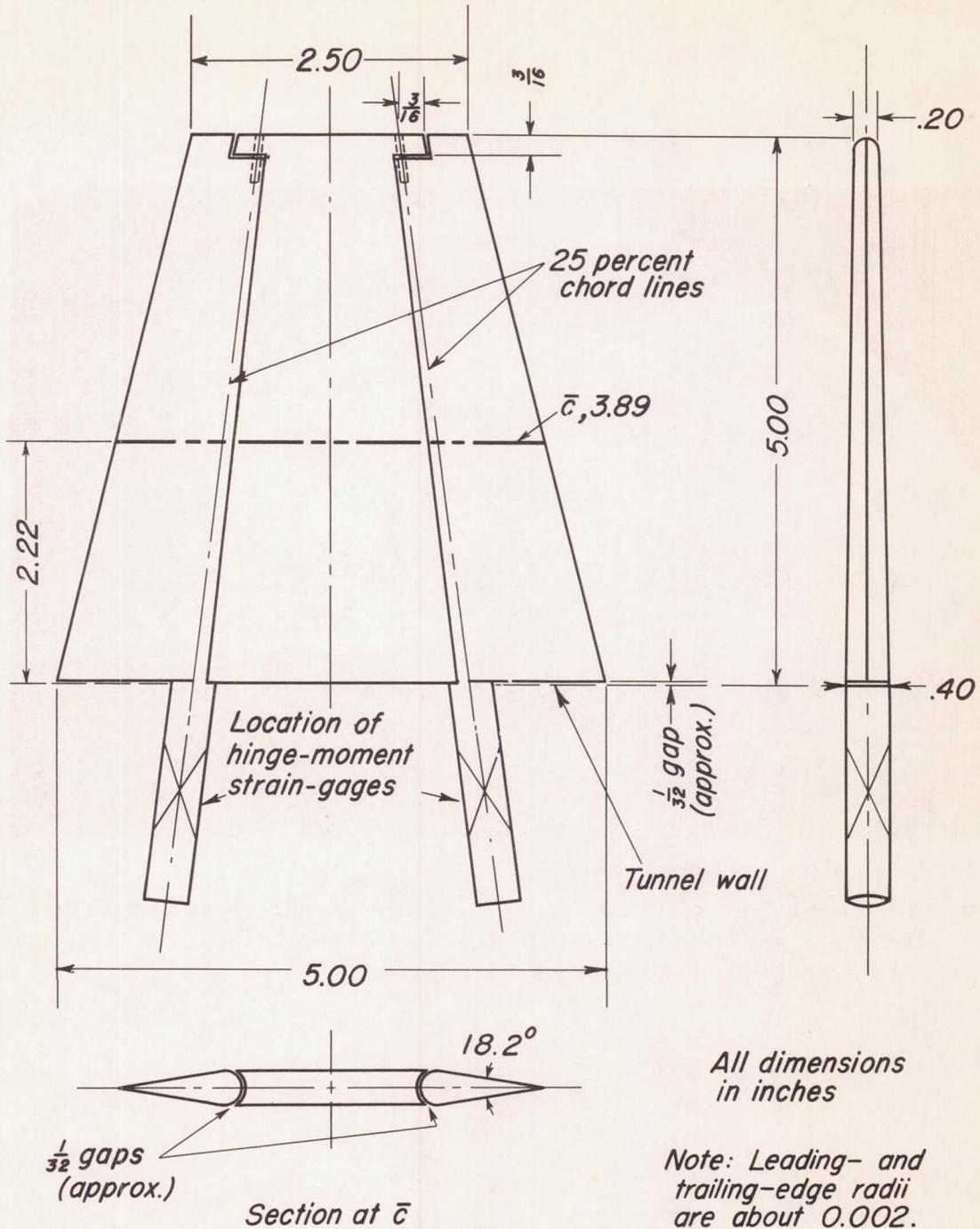
Figure 2.— Sketch of the semispan wing model with leading- and trailing-edge flaps.
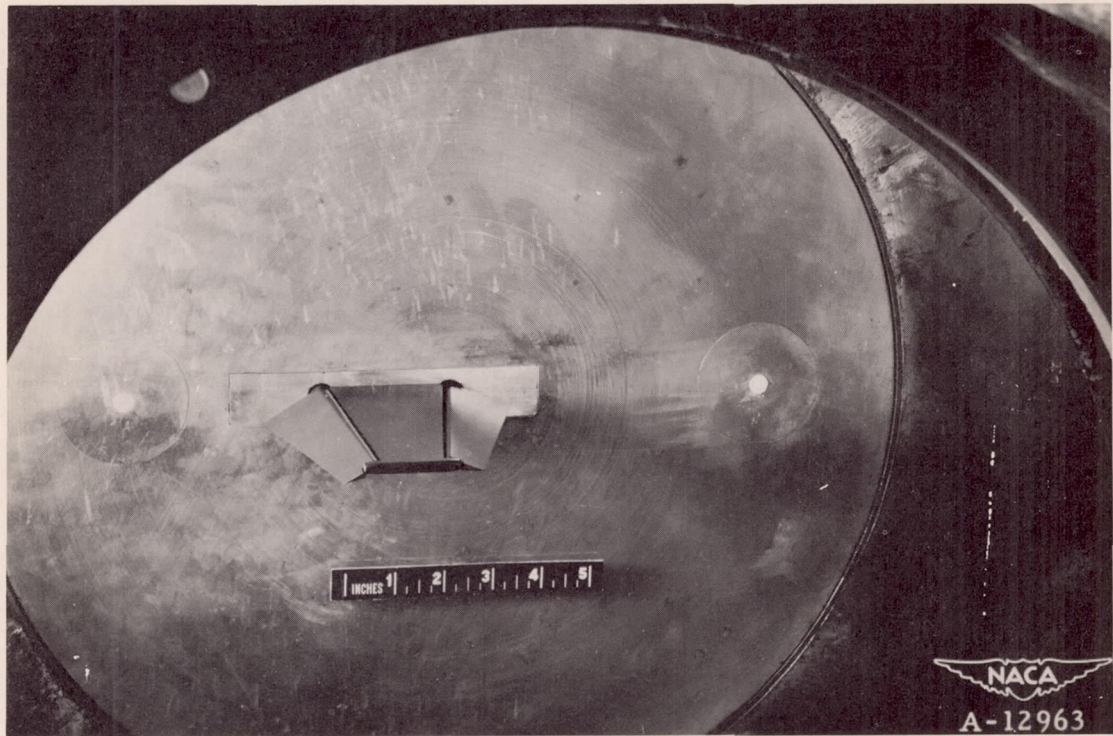
Figure 3.— Photograph of the model, with the leading— and trailing—
edge flaps deflected, mounted on the semispan balance in the Ames
1— by 3–1/2–foot high–speed wind tunnel.
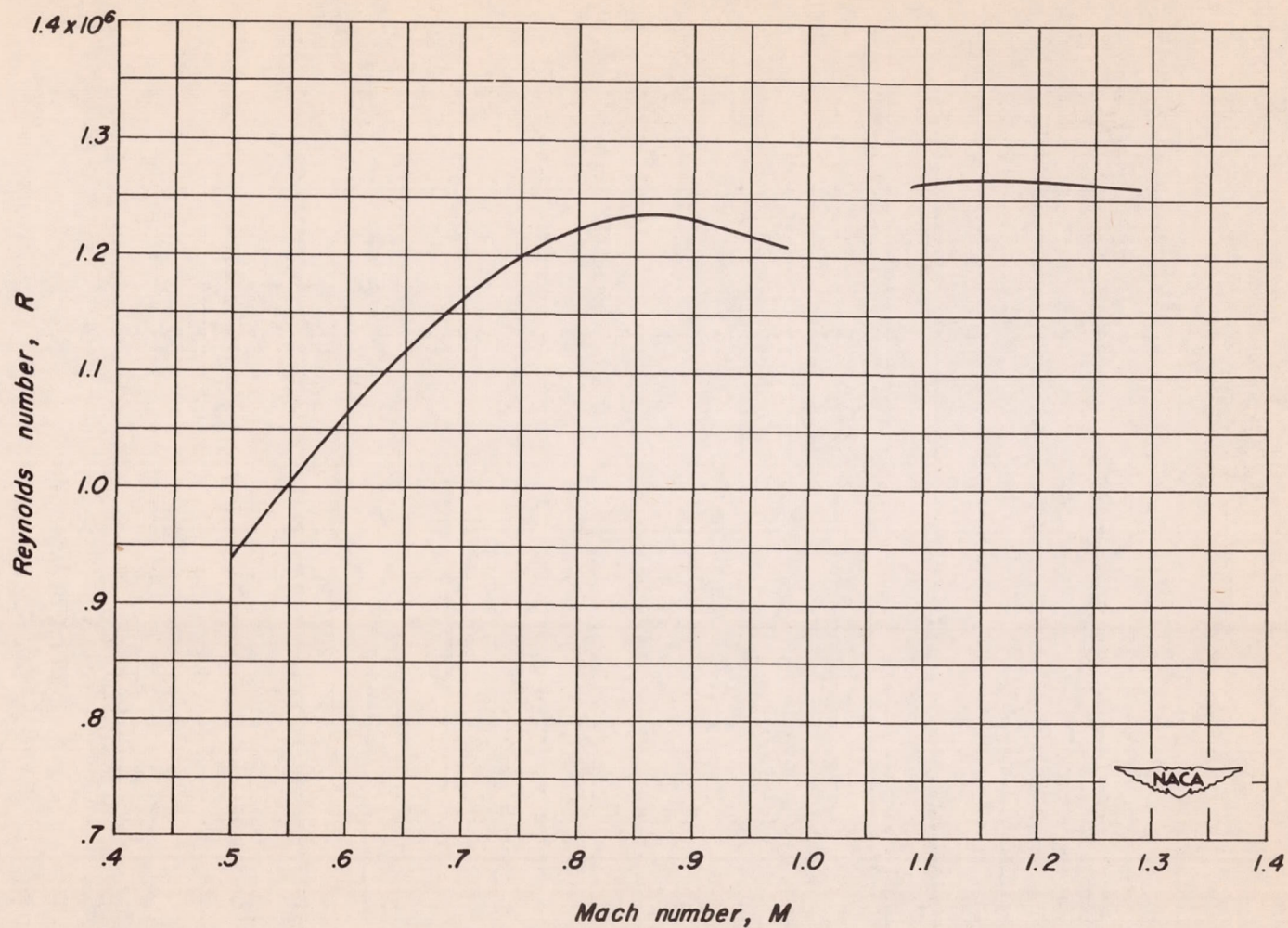
Figure 4.– Nominal variation of Reynolds number with Mach number for tests of the semispan wing of aspect ratio 2.67 in the Ames 1– by $3\frac{1}{2}$–foot high–speed wind tunnel.
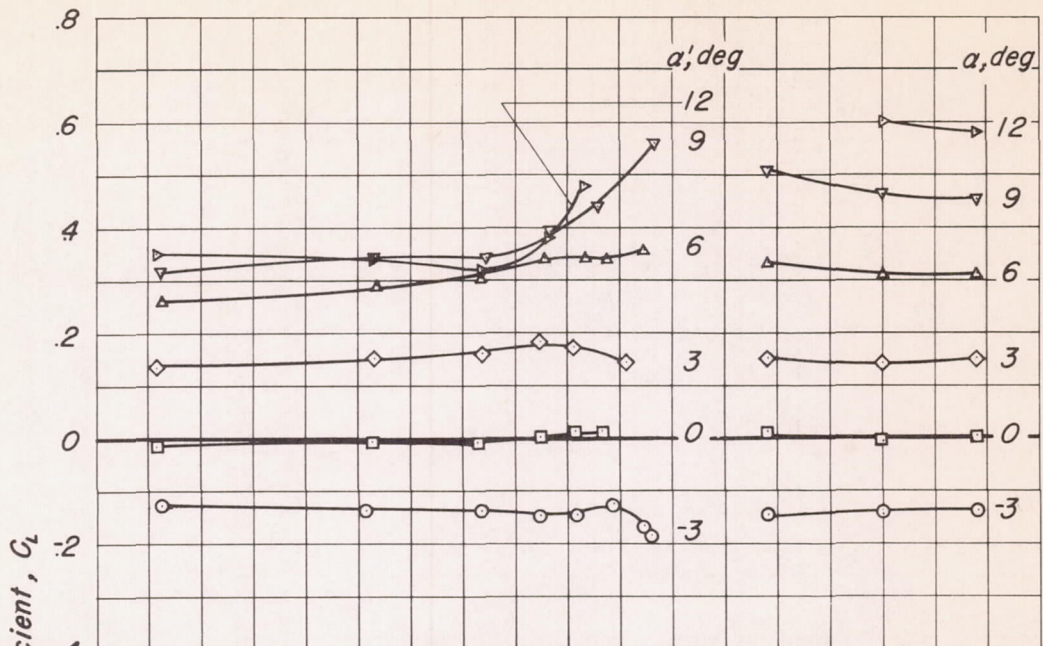
(a) Gaps unsealed.
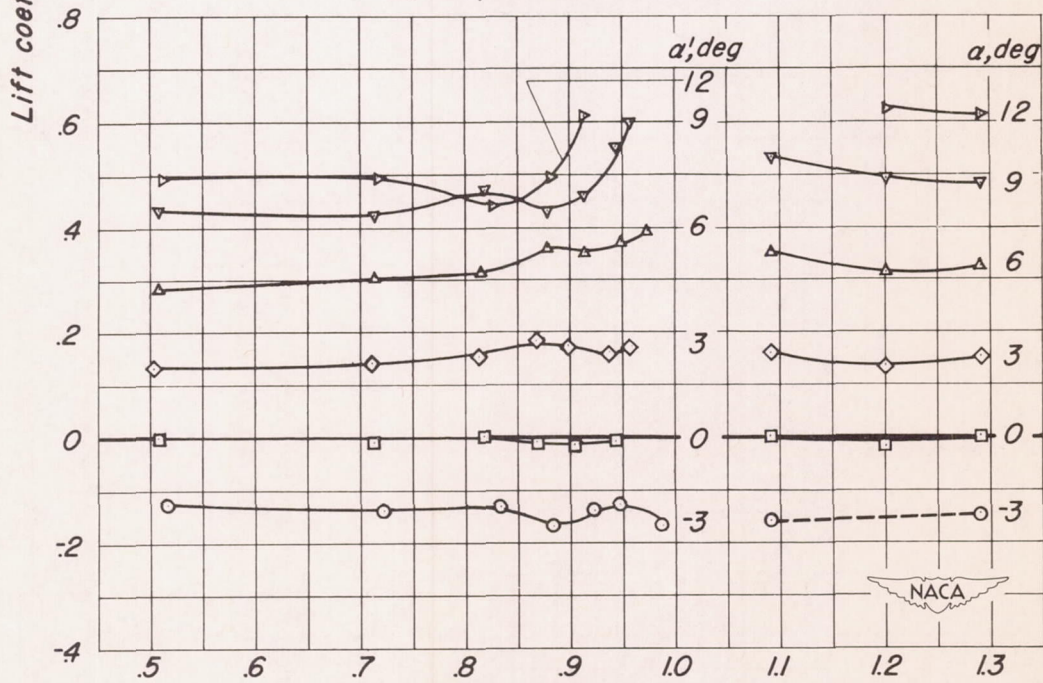
(b) Gaps sealed.

Figure 5.— Variation of lift coefficient with Mach number for various geometric angles of attack, flaps undeflected.

M=.5   .8   .9   .95   1.09   1.20   1.29

Lift coefficient, C_L

$\delta_n°$	$\delta_t°$		$\delta_n°$	$\delta_t°$
0°	0°		-5°	10°
5°	10°		-10°	20°
10°	20°		-20°	60°

Angle of attack, α, deg
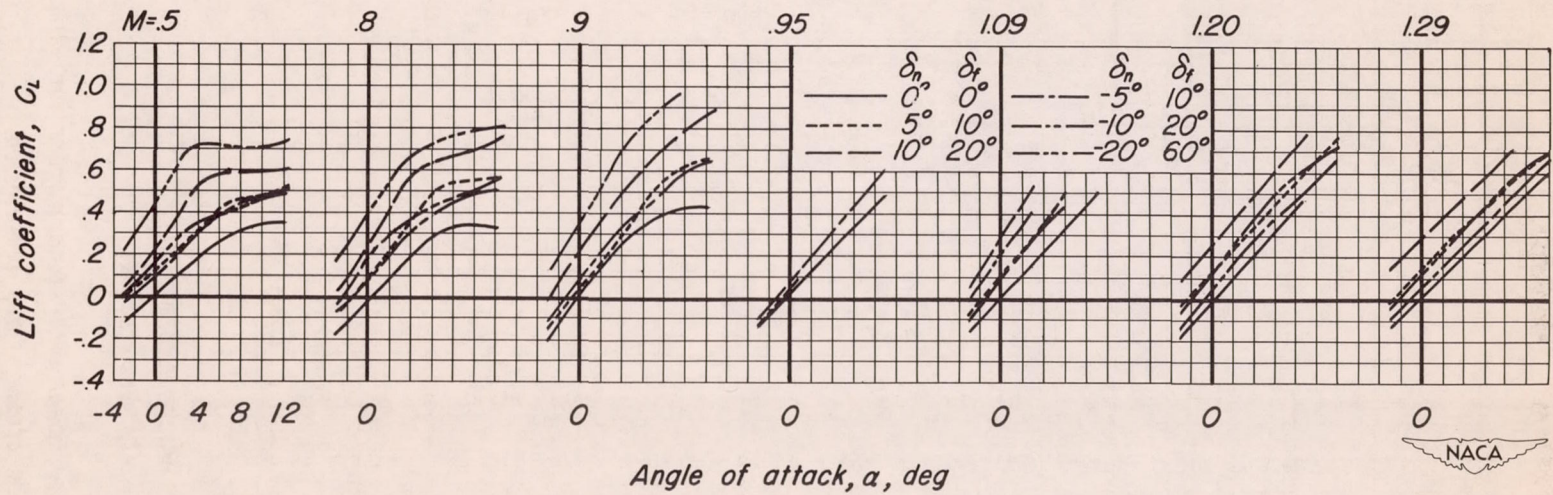
Figure 6.– Variation at several Mach numbers of lift coefficient with angle of attack for various combinations of leading– and trailing–edge flap deflections, gaps unsealed.

(a) Leading-edge flap deflected, trailing-edge flap undeflected (data from reference 5).

(b) Trailing-edge flap deflected, leading-edge flap undeflected (data from reference 6).
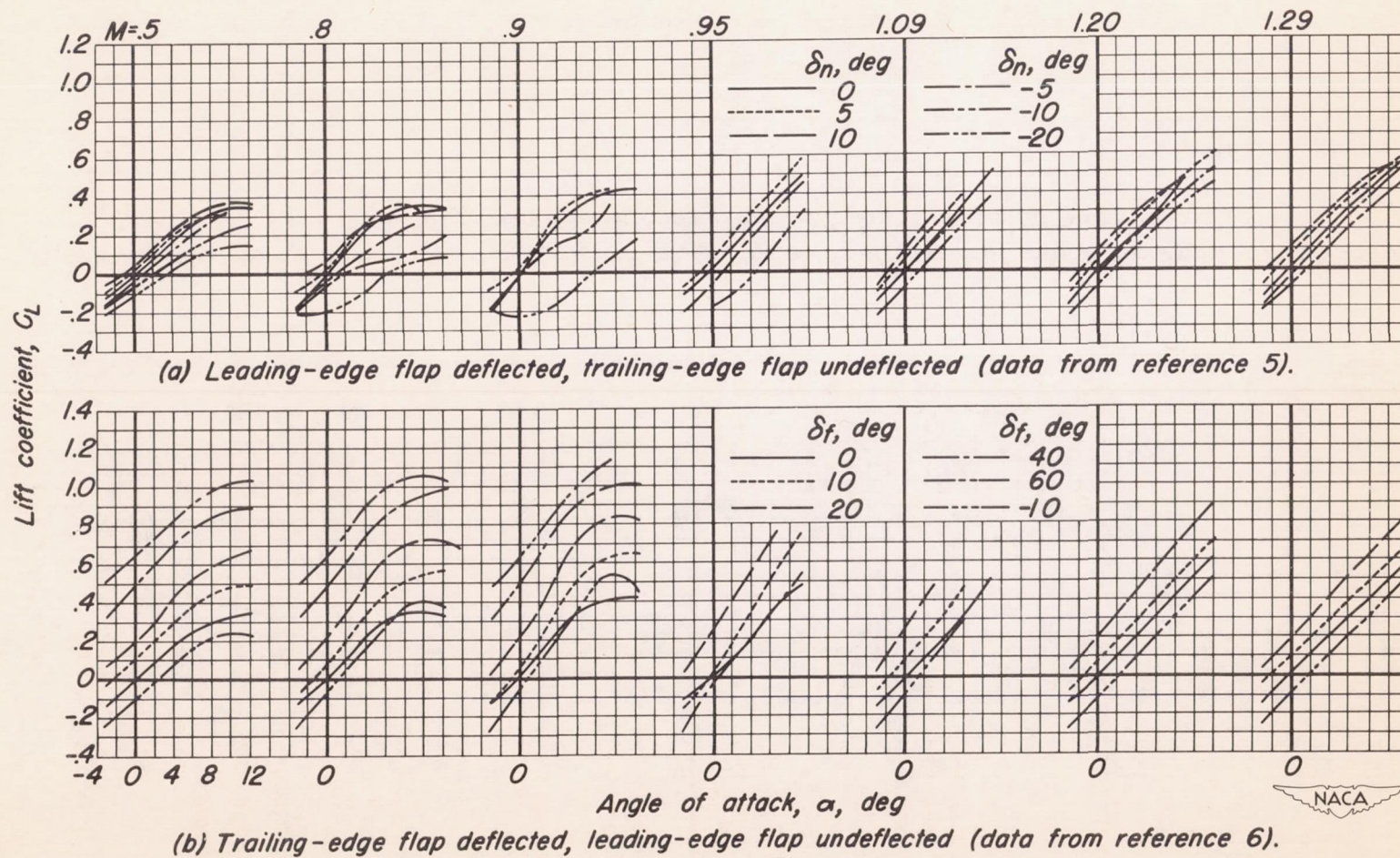
Figure 7.- Variation at several Mach numbers of lift coefficient with angle of attack for separate deflections of the leading-and trailing-edge flaps, gaps unsealed.
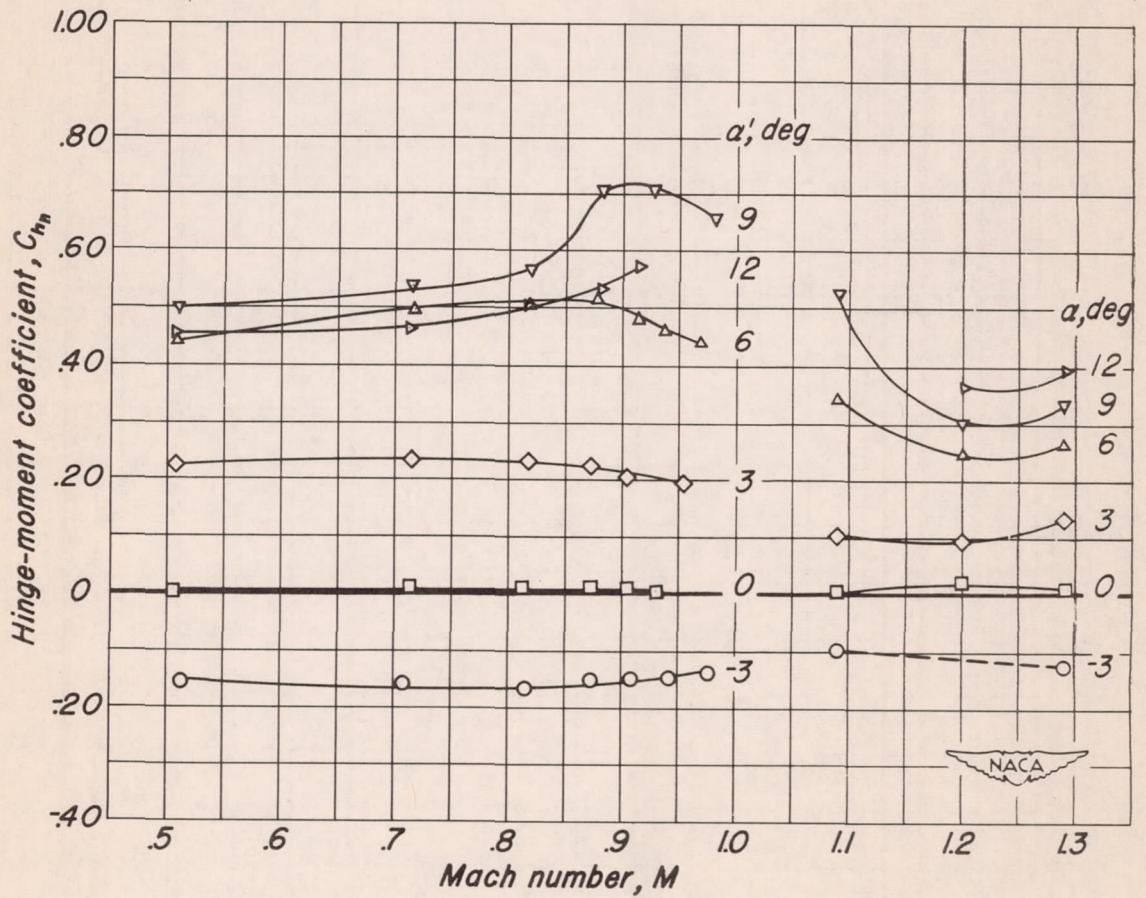
Figure 8.— Variation with Mach number of the hinge-moment coefficient of the leading-edge flap for various geometric angles of attack; flaps undeflected, gaps unsealed.
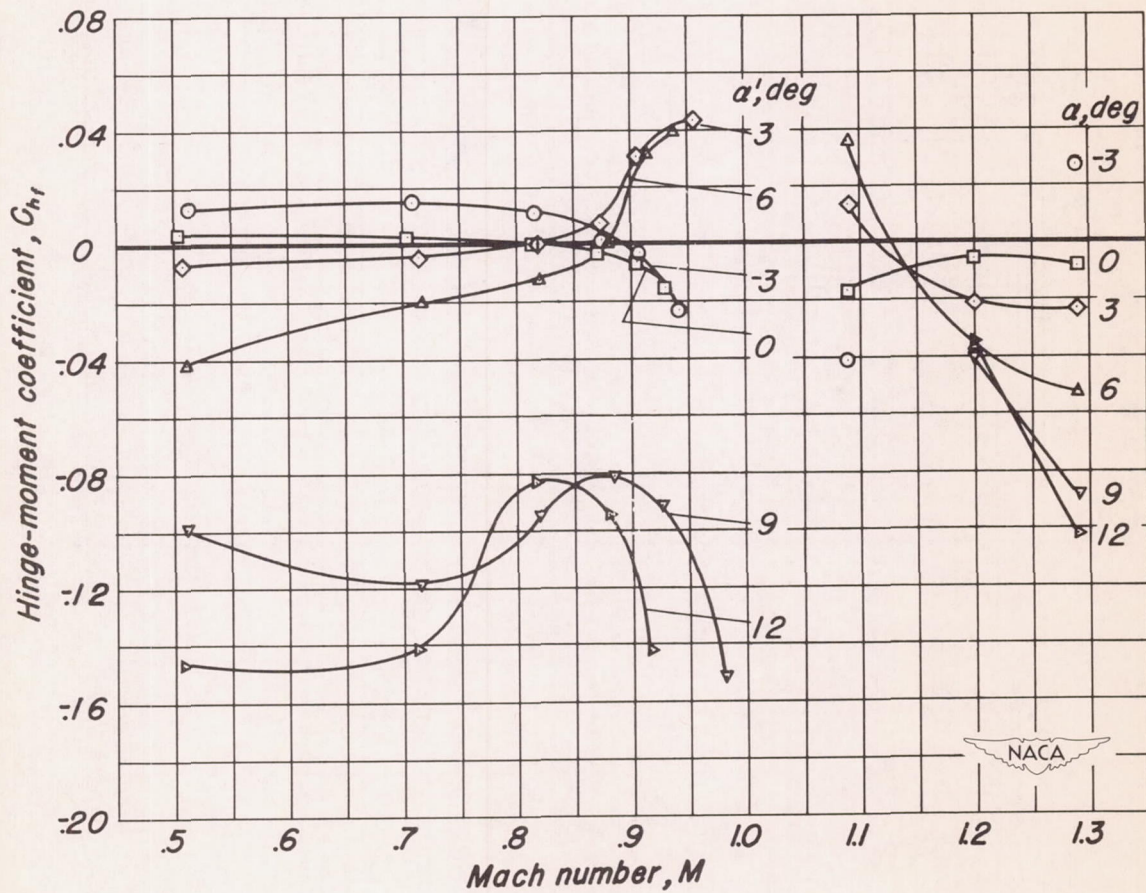
Figure 9.— Variation with Mach number of the hinge-moment coefficient of the trailing-edge flap for various geometric angles of attack; flaps undeflected, gaps unsealed.

Hinge-moment coefficient, C_{h_n}

M=.5   .8   .9   .95   1.09   1.20   1.29

1.2
.8
.4
0
-.4
-.8
-1.2
-4 0 4 8 12   0   0   0   0   0   0

Angle of attack, a, deg

(a) Leading-edge flap.

Hinge-moment coefficient, C_{h_f}

M=.5   .8   .9   .95   1.09   1.20   1.29

δ_n	δ_f		δ_n	δ_f
0°	0°		-5°	10°
5°	10°		-10°	20°
10°	20°		-20°	60°

1.2
.8
.4
0
-.4
-.8
-1.2
-4 0 4 8 12   0   0   0   0   0   0

Angle of attack, a, deg

(b) Trailing-edge flap.

NACA
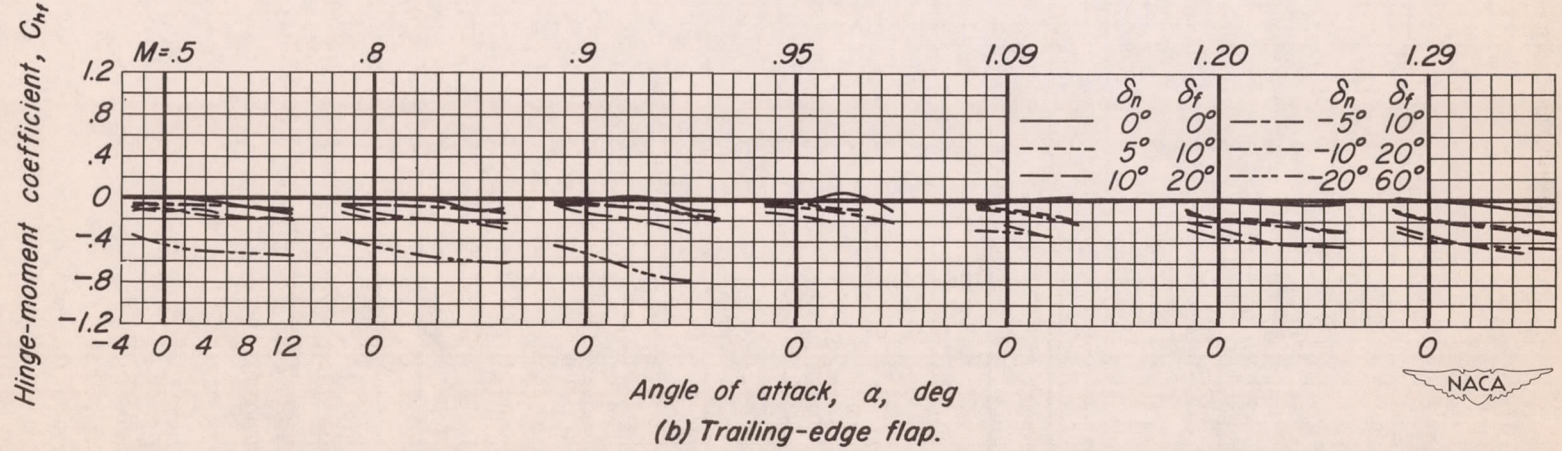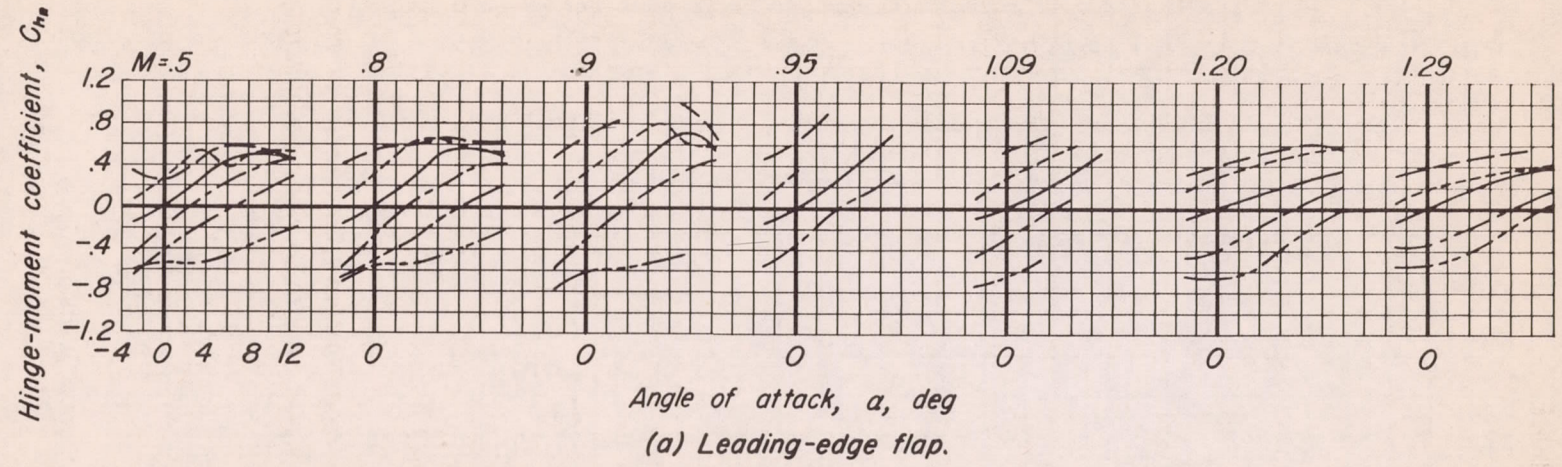
Figure 10.- Variation at several Mach numbers of leading- and trailing-edge-flap hinge-moment coefficients with angle of attack for various combinations of leading- and trailing-edge-flap deflections, gaps unsealed.
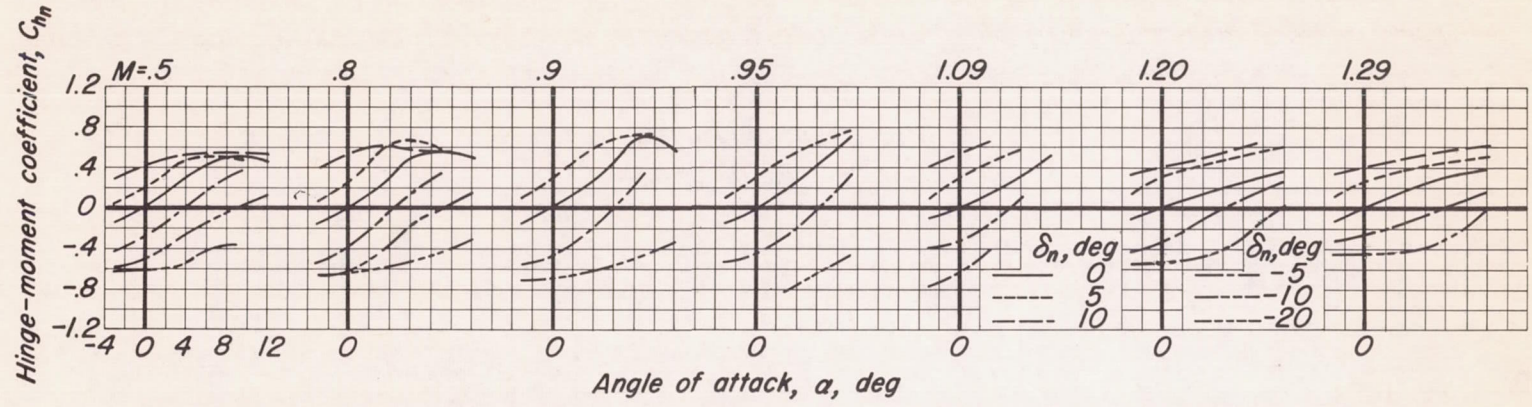
(a) Leading-edge flap deflected, trailing-edge flap undeflected (data from reference 5).
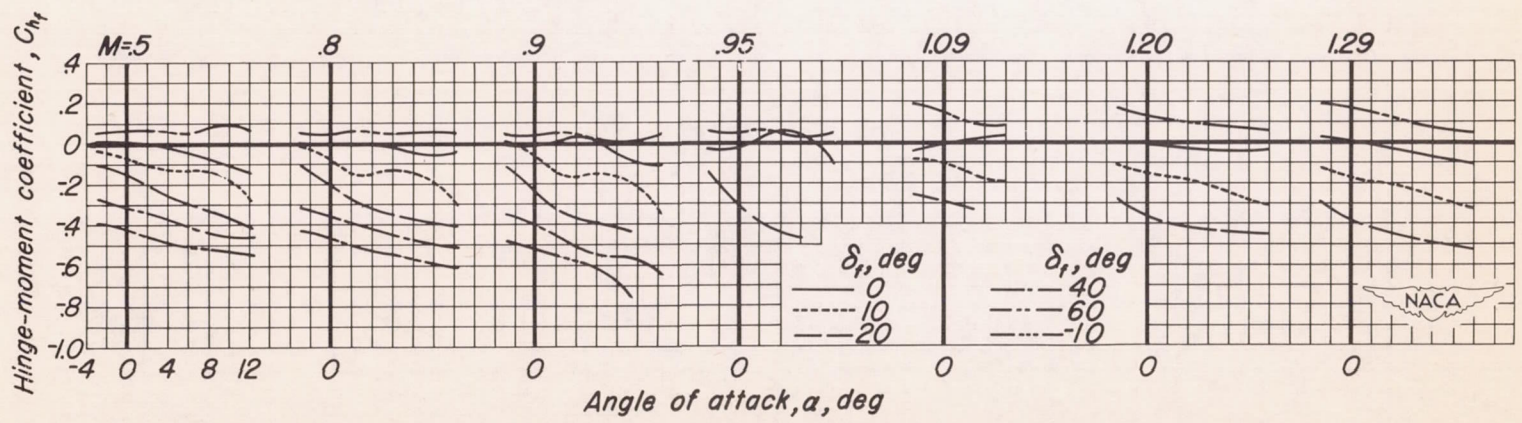
(b) Trailing-edge flap deflected, leading-edge flap undeflected (data from reference 6).

Figure 11.— Variation at several Mach numbers of hinge-moment coefficient with angle of attack for the leading- and trailing-edge flaps deflected separately, gaps unsealed.
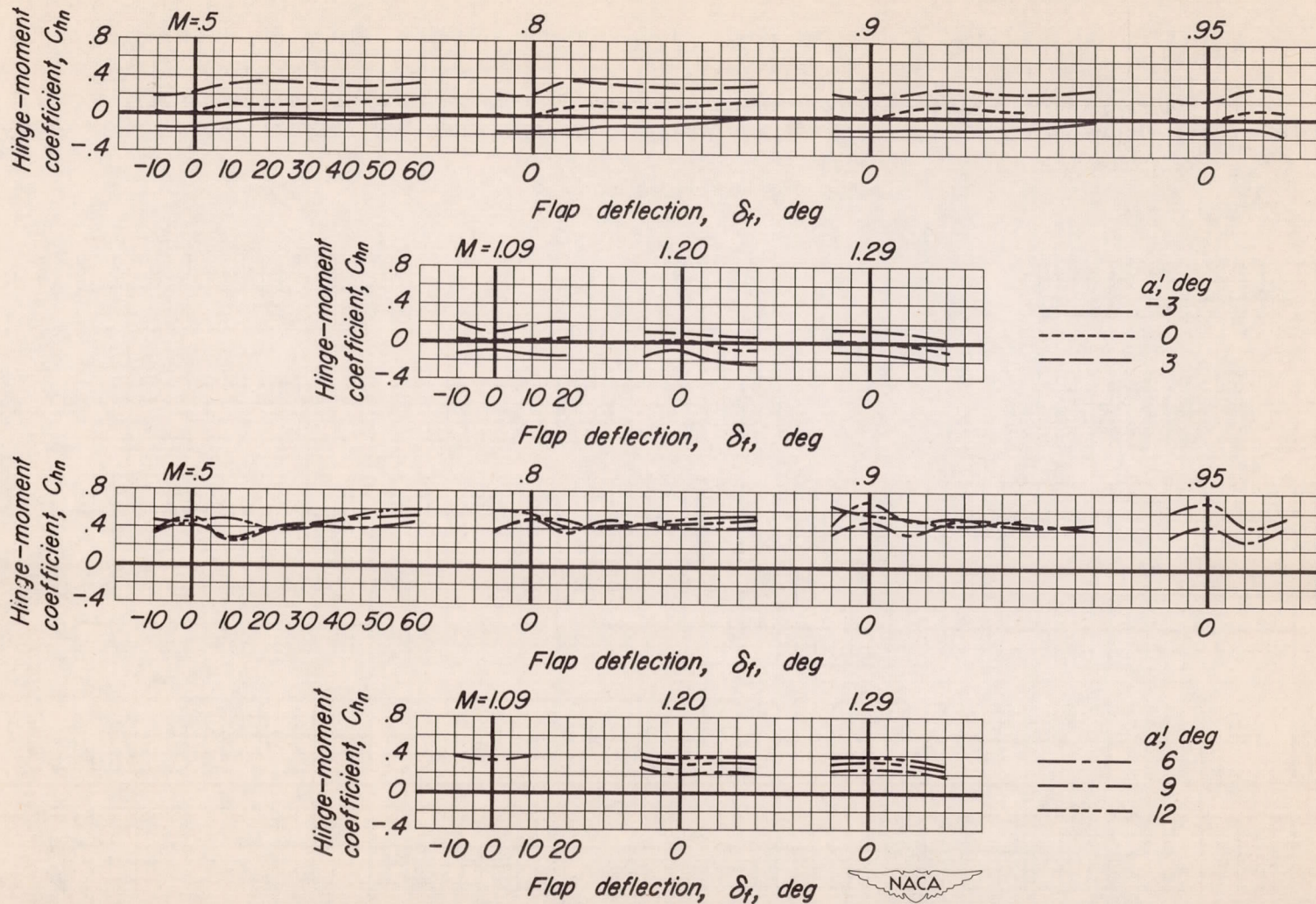
Figure 12.- Effect of trailing-edge-flap deflection at several Mach numbers on the hinge-moment coefficient of the undeflected leading-edge flap for various geometric angles of attack, gaps unsealed.
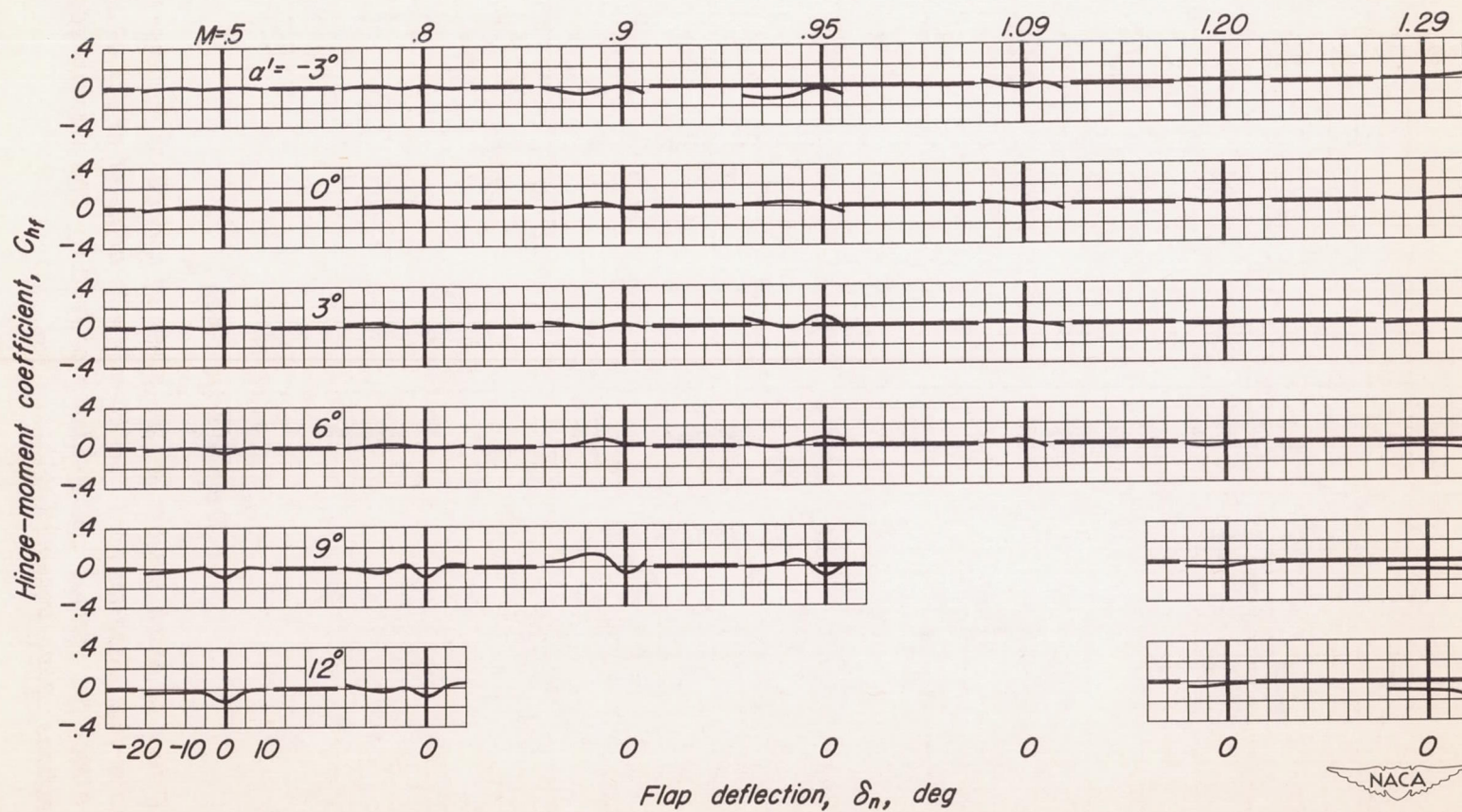
Figure 13.- Effect of leading-edge-flap deflection at several Mach numbers on the hinge-moment coefficient of the undeflected trailing-edge flap for various geometric angles of attack, gaps unsealed.
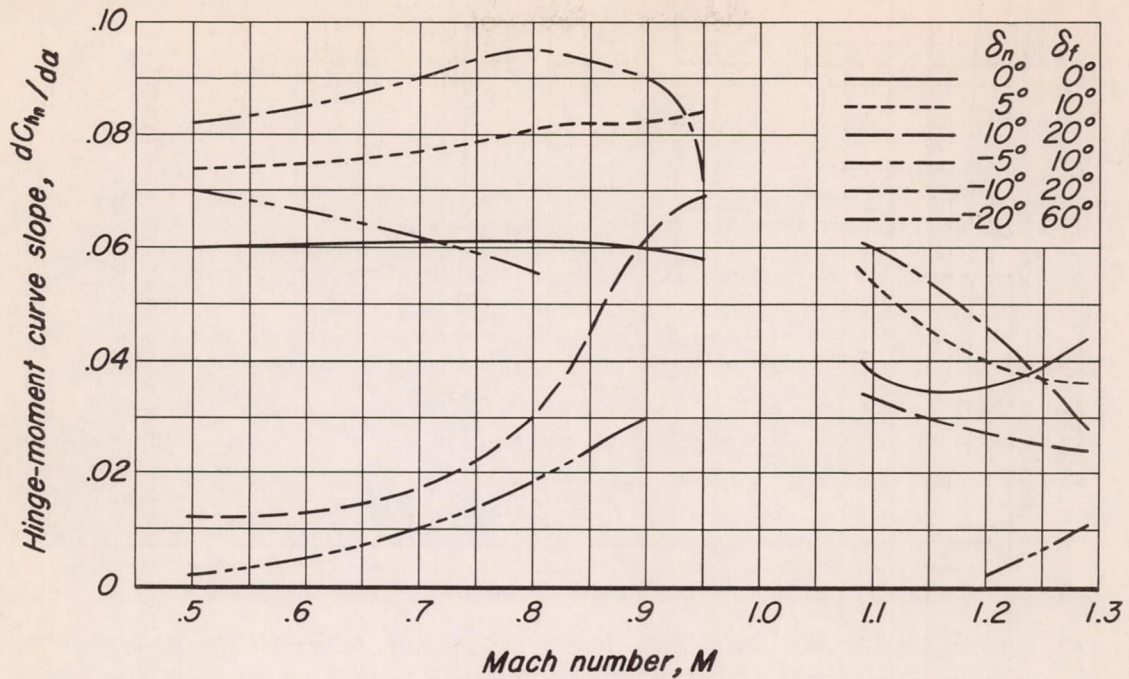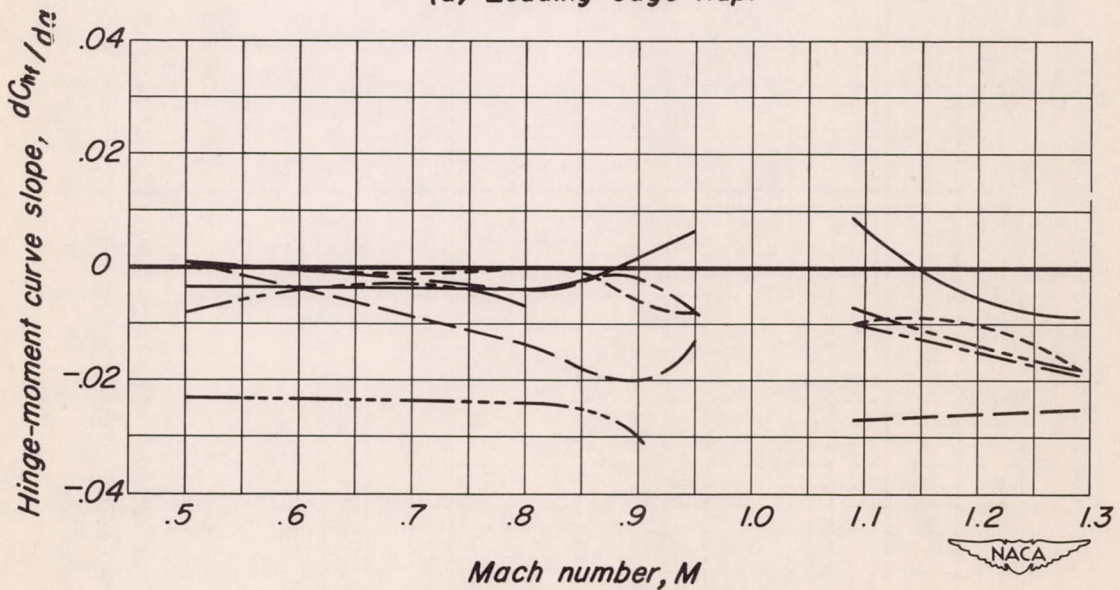
Figure 14.- Effect of Mach number on the rates of change of leading- and trailing-edge-flap hinge-moment coefficients with angle of attack at zero angle of attack for various combinations of leading- and trailing-edge-flap deflections, gaps unsealed.
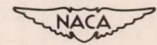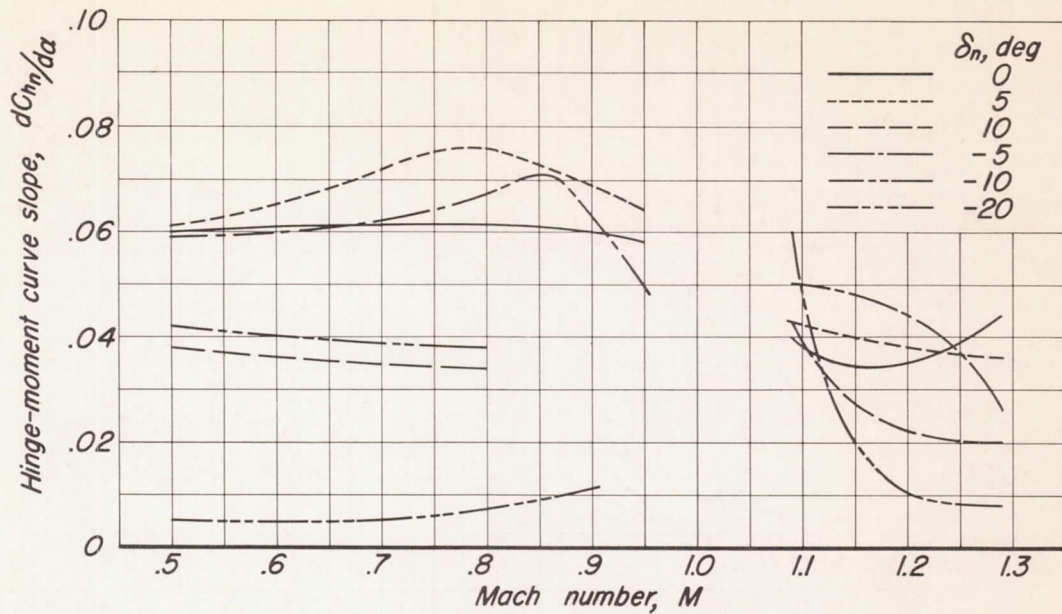
(a) Leading-edge flap deflected, trailing-edge flap undeflected (data from reference 5).
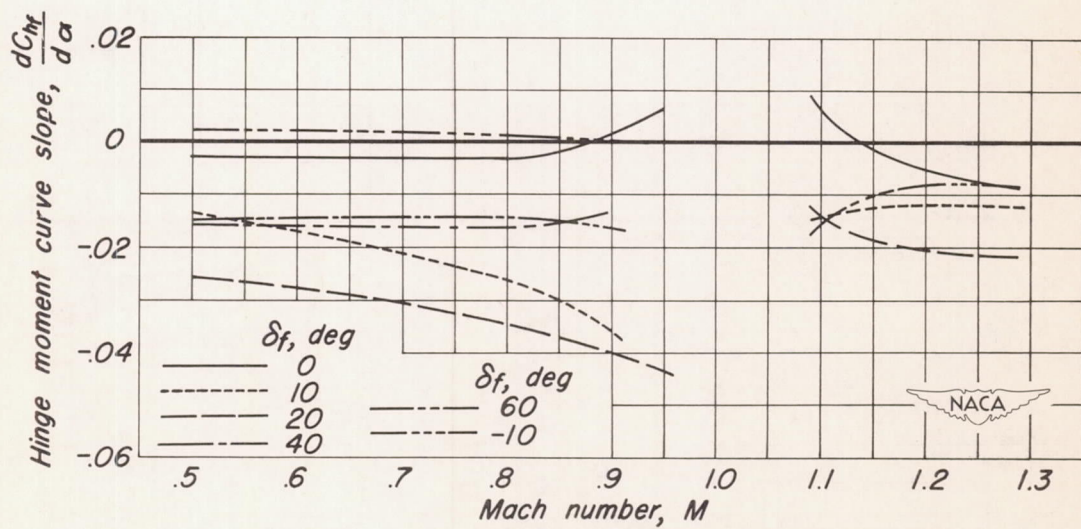
(b) Trailing-edge flap deflected, leading-edge flap undeflected (data from reference 6).

Figure 15.— Effect of Mach number on the rates of change of leading- and trailing-edge-flap hinge-moment coefficients with angle of attack at zero angle of attack for separate deflections of the flaps, gaps unsealed.
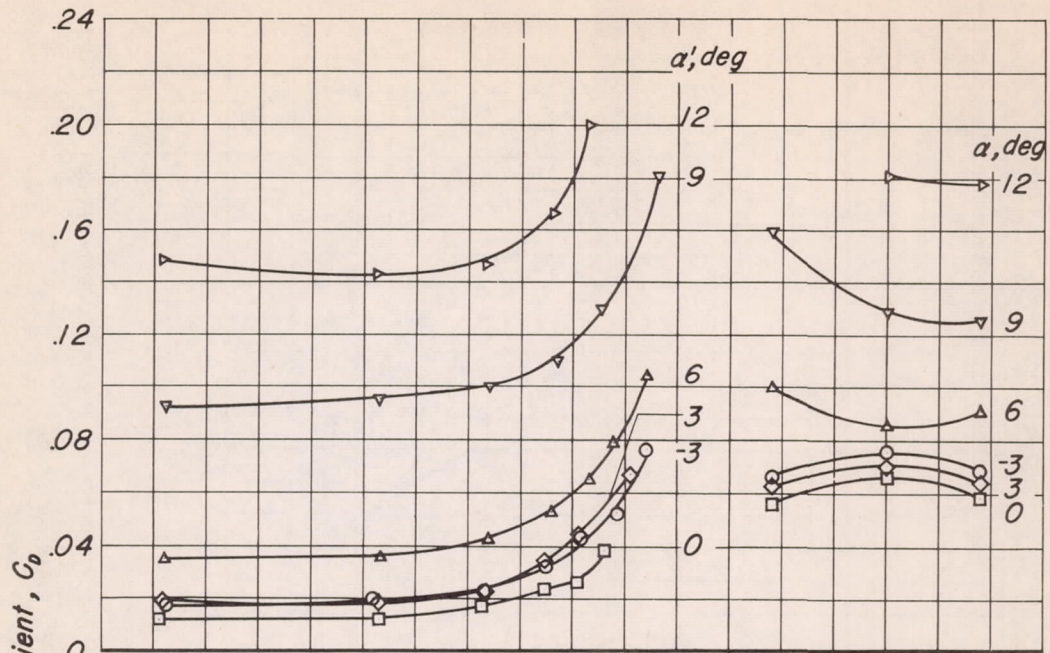
(a) Gaps unsealed.
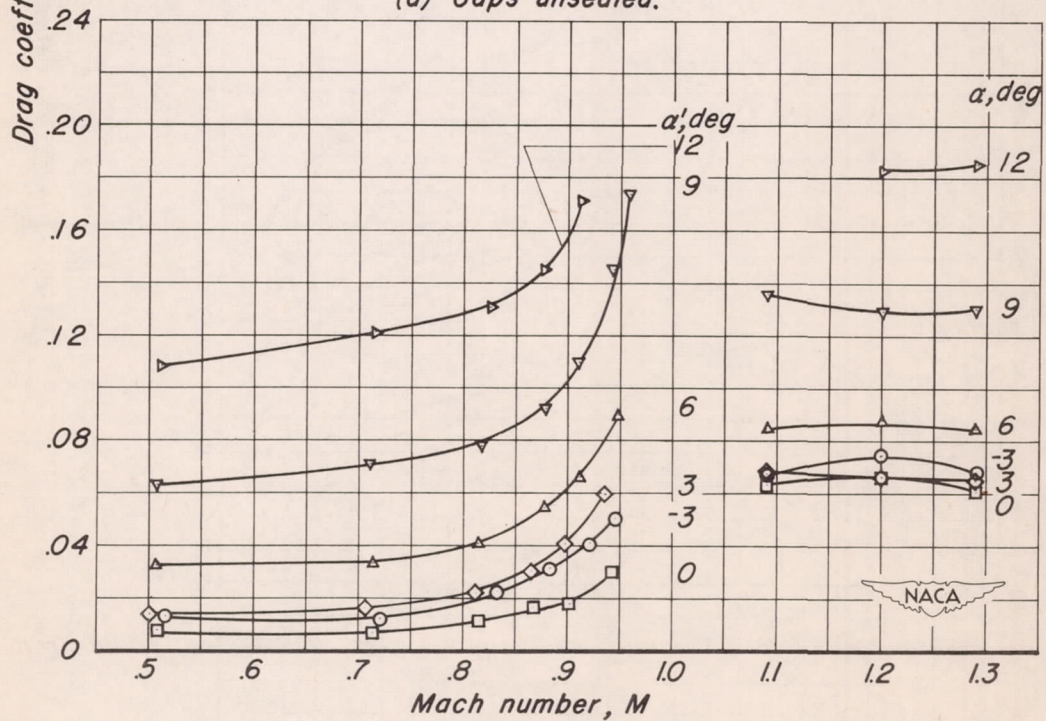
(b) Gaps sealed.

Figure 16.— Variation of drag coeft   ch number for various geometric
                    angles of at.   teflected.
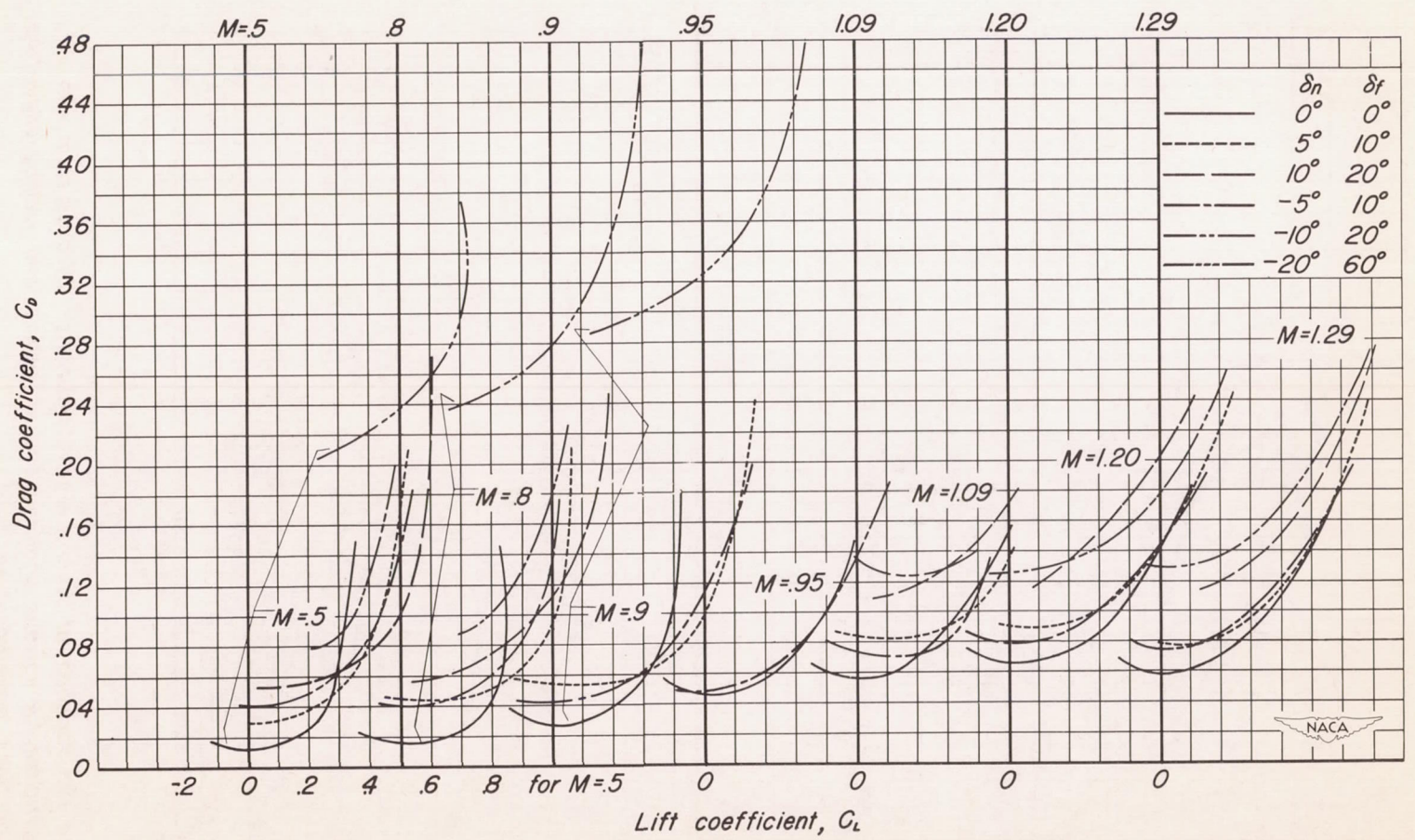
Figure 17.- Variation at several Mach numbers of drag coefficient with lift coefficient for various combinations of leading-
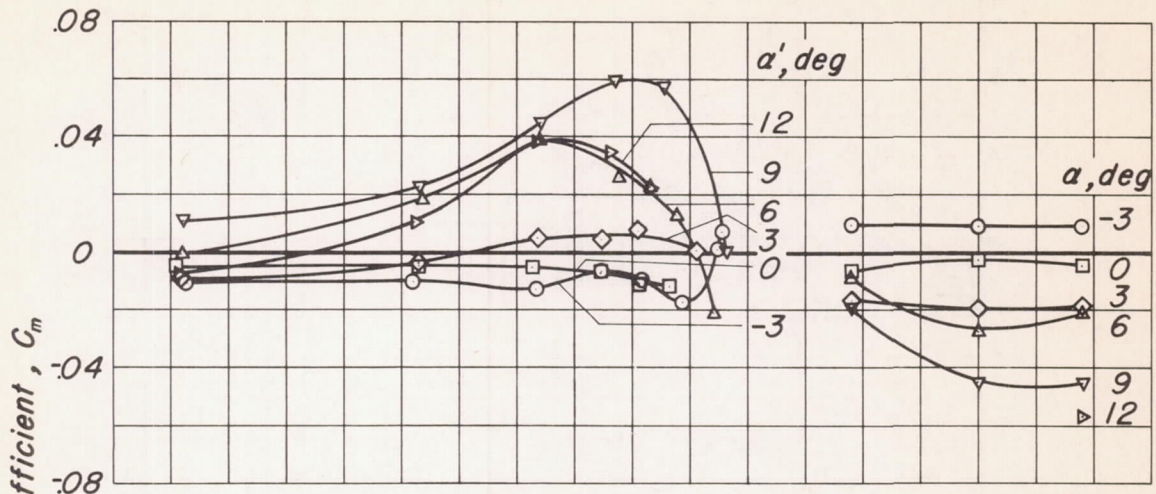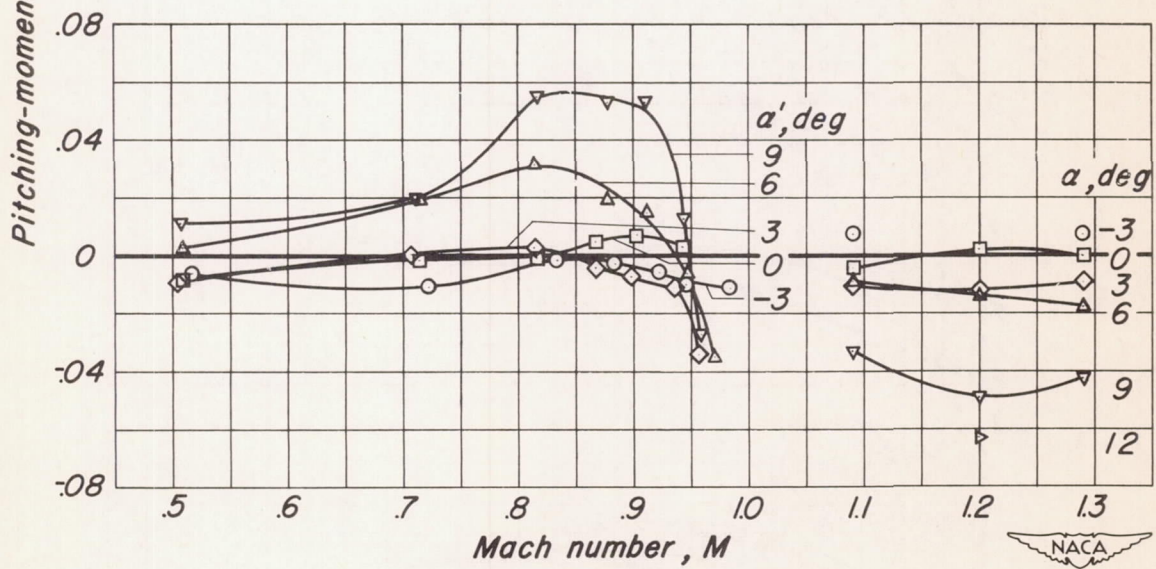and trailing-edge-flap deflections, gaps unsealed.
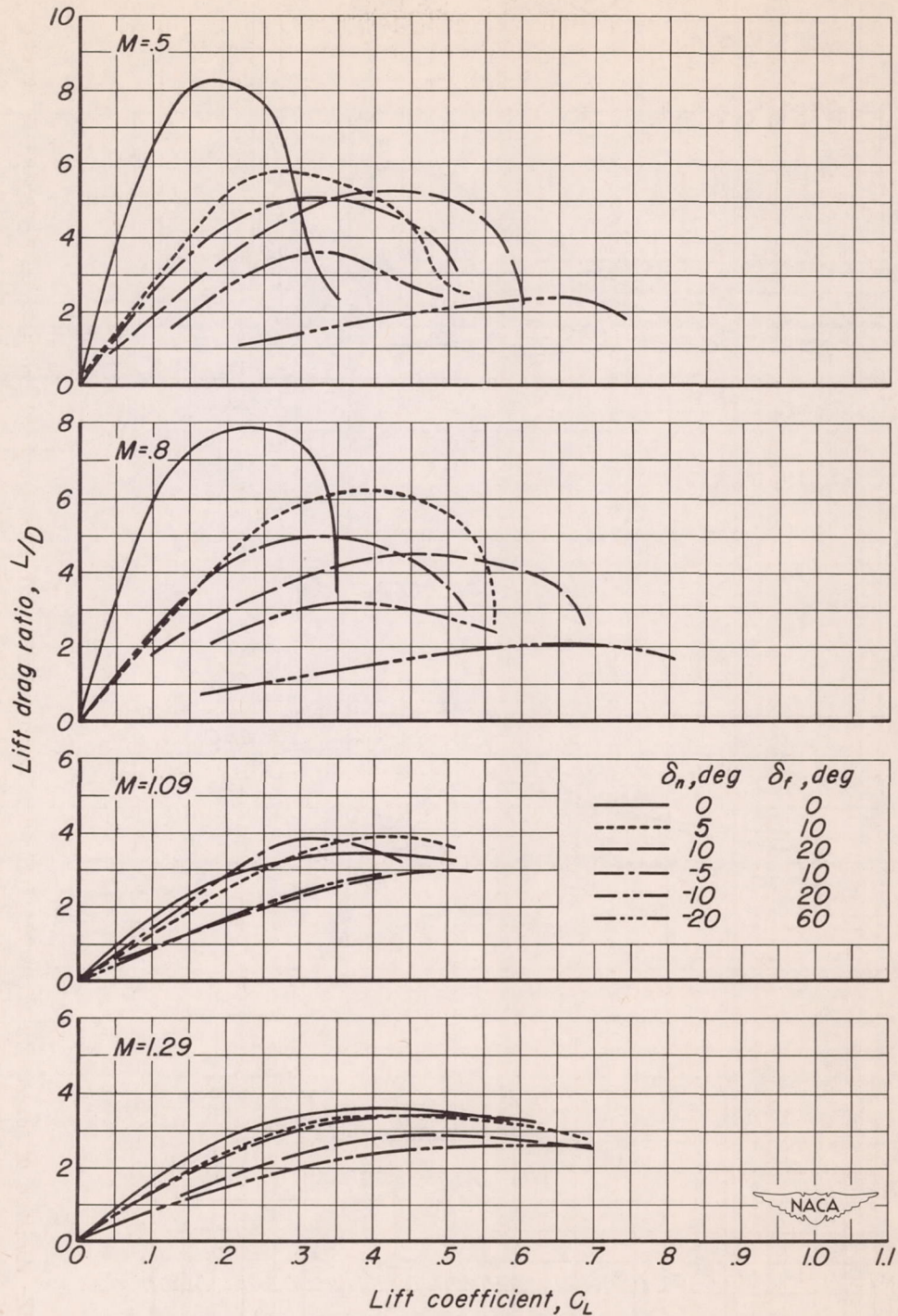
Figure 18.- Variation at several Mach numbers of lift-drag ratio with lift coefficient for various combinations of leading- and trailing-edge-flap deflections, gaps unsealed.

(a) Gaps unsealed.

(b) Gaps sealed.

Figure 19.— Variation of pitching—moment coefficient with Mach number for various geometric angles of attack, flaps undeflected.
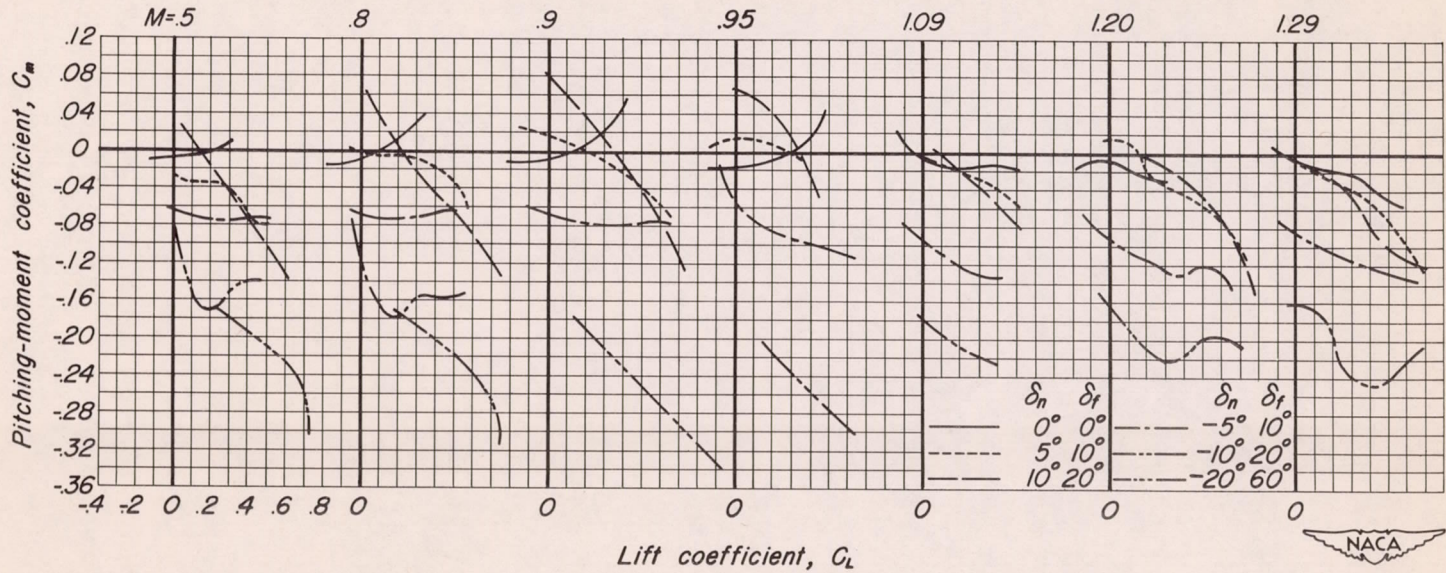
Figure 20.- Variation at several Mach numbers of pitching-moment coefficient with lift coefficient for various combinations of leading- and trailing-edge-flap deflections, gaps unsealed.